Atmospheric Environment 158 (2017) 11–26

Contents lists available at ScienceDirect

Atmospheric Environment

journal homepage: www.elsevier.com/locate/atmosenv

Investigating African trace gas sources, vertical transport, and oxidation using IAGOS-CARIBIC measurements between Germany and South Africa between 2009 and 2011

U.R. Thorenz [a, *], A.K. Baker [a], E.C. Leedham Elvidge [b], C. Sauvage [a], H. Riede [a], P.F.J. van Velthoven [c], M. Hermann [d], A. Weigelt [d, e], D.E. Oram [f], C.A.M. Brenninkmeijer [a], A. Zahn [g], J. Williams [a]

[a] Max Planck Institute for Chemistry, Mainz, Germany
[b] School of Environmental Sciences, University of East Anglia, Norwich, UK
[c] Royal Netherlands Meteorological Institute (KNMI), De Bilt, The Netherlands
[d] Leibniz Institute for Tropospheric Research, Leipzig, Germany
[e] now Federal Maritime and Hydrographic Agency, Hamburg, Germany
[f] National Centre for Atmospheric Science, University of East Anglia, Norwich, UK
[g] Karlsruhe Institute of Technology, Karlsruhe, Germany

HIGHLIGHTS

- Trace gases were measured in 10–12 km on transects from Germany to South Africa.
- Mixing ratios show convection is the dominant transport pattern.
- Source apportionment methods show biomass burning and background air as sources.
- Northern hemisphere air masses are diluted with air containing long lived NMHCs.
- Ozone production in biomass burning outflow in the northern hemisphere.

ARTICLE INFO

Article history:
Received 30 September 2016
Received in revised form
9 March 2017
Accepted 11 March 2017
Available online 16 March 2017

Keywords:
Africa
Biomass burning
NMHC
Trace gas emissions
UTLS
Aircraft observation

ABSTRACT

Between March 2009 and March 2011 a commercial airliner equipped with a custom built measurement container (IAGOS-CARIBIC observatory) conducted 13 flights between South Africa and Germany at 10–12 km altitude, traversing the African continent north-south. In-situ measurements of trace gases (CO, CH_4, H_2O) and aerosol particles indicated that strong surface sources (like biomass burning) and rapid vertical transport combine to generate maximum concentrations in the latitudinal range between 10°N and 10°S coincident with the inter-tropical convergence zone (ITCZ). Pressurized air samples collected during these flights were subsequently analyzed for a suite of trace gases including C_2-C_8 non-methane hydrocarbons (NMHC) and halocarbons. These shorter-lived trace gases, originating from both natural and anthropogenic sources, also showed near equatorial maxima highlighting the effectiveness of convective transport in this region. Two source apportionment methods were used to investigate the specific sources of NMHC: positive matrix factorization (PMF), which is used for the first time for NMHC analysis in the upper troposphere (UT), and enhancement ratios to CO. Using the PMF method three characteristic airmass types were identified based on the different trace gas concentrations they obtained: biomass burning, fossil fuel emissions, and "background" air. The first two sources were defined with reference to previously reported surface source characterizations, while the term "background" was given to air masses in which the concentration ratios approached that of the lifetime ratios. Comparison of enhancement ratios between NMHC and CO for the subset of air samples that had experienced recent contact with the planetary boundary layer (PBL) to literature values showed that the burning of savanna and tropical forest is likely the main source of NMHC in the African upper troposphere (10–12 km). Photochemical aging patterns for the samples with PBL contact revealed that the air had different degradation histories depending on the hemisphere in which they were emitted. In the southern

* Corresponding author.
E-mail address: ute.thorenz@mpic.de (U.R. Thorenz).

http://dx.doi.org/10.1016/j.atmosenv.2017.03.021

hemisphere (SH) air masses experienced more dilution by clean background air whereas in the northern hemisphere (NH) air masses are less diluted or mixed with background air still containing longer lived NMHC. Using NMHC photochemical clocks ozone production was seen in the BB outflow above Africa in the NH.

1. Introduction

Although only 16% of the world population lives in Africa and industrialization is low, its geographical position across the southern and northern subtropics; the frequent occurrence of lightning and wild fires; its vast savannas and tropical forests and the seasonal migration of the inter-tropical convergence zone (ITCZ), all render this continent of considerable interest and importance for the chemistry of the global atmosphere. Particularly important emissions come from vegetation and soils (e.g.Guenther et al., 1996; Scholes and Andreae, 2000; Tubiello et al., 2013), the burning of biomass such as tropical savannas or forests (e.g. Blake et al., 1996; Swap et al., 2003), emissions associated with fossil fuel usage (e.g. Anomohanran, 2012), pollution from domestic cooking, and even the growing number of megacities (Hopkins et al., 2009; Karl et al., 2009). Due to the seasonal north-south transition of the ITCZ over Africa, these emissions may impact either hemisphere (Crutzen and Andreae, 1990). Vertical transport processes, which are particularly effective in the tropics, then act to transport these emissions from the planetary boundary layer (PBL) to the upper troposphere (UT). These processes include: convective transport within the ITCZ (Andreae et al., 2001; Sauvage et al., 2007; Waliser and Gautier, 1993); convection associated with variations in the southern branch of the African Easterly Jet (Mari et al., 2008), and the mid-to upper-tropospheric transport from Central Africa to the southern Atlantic Ocean (Real et al., 2010). The vigorous convective transport from the PBL to the UT, the strong emission sources and the active photochemistry associated with high radiation make the African UT a particularly interesting location to study atmospheric composition and processing. Moreover, due to logistical, political, and technical constraints, the tropical African UT is considerably less well studied than the UT at temperate latitudes over America and Europe.

Several previous studies have investigated BB emissions and the photochemistry of trace gases from the African continent. TRACE-A (Transport and Atmospheric Chemistry near the Equator-Atlantic) and SAFARI-92 (Southern African Fire-Atmosphere Research Initiative) both investigated high ozone (O_3) concentrations above the South Atlantic Ocean between August and October, which were discovered in the mid-1980s by satellite measurements. Both campaigns concluded that BB in South Africa was the cause of the seasonal enhanced O_3 levels (Fishman et al., 1996; Swap et al., 2003). SAFARI 2000 (the Southern African Regional Science Initiative) focused on the optical and radiative effects of BB plumes from southern Africa (Laakso et al., 2008) whereas the multidisciplinary approach of the AMMA program (African Monsoon Multidisciplinary Analysis) focused on the West African Monsoon. Within this program, organic trace gases from BB emission plumes in both the upper and mid troposphere (Bechara et al., 2010; Haywood et al., 2008) were detected and related to O_3 photochemistry (Real et al., 2010).

Here we present a unique atmospheric measurement dataset encompassing multiple north-south transects of the African continent at 10–12 km altitude between March 2009 and March 2011. The measurements were made by the IAGOS-CARIBIC observatory (Civil Aircraft for the Regular Investigation of the atmosphere Based on an Instrument Container; www.caribic-atmospheric.com) on flights by a Lufthansa Airbus A340-600 between Frankfurt, Germany and Cape Town or Johannesburg, South Africa. All the aforementioned campaigns have focused on specific sections of the African continent, in this study we provide an investigation of trace gas transport and processing on the continental scale from 35 °N to 35 °S.

The data are exploited to investigate the sources, transport and photochemistry of trace gases emitted from Africa reaching the UT. Non-methane hydrocarbons (NMHC) have been used to investigate sources using both emission ratio comparisons and a positive matrix factorization (PMF) model. This source receptor model works with direct measurement data so that both the source spatial pattern and emission quantity could be ascertained statistically from the measurement data without reference to emission inventories. Photochemical processing was also assessed by examining NMHC based photochemical clocks. The chemical fate of the exported trace gases was then traced using NMHC ratios. In the UT NMHC are primarily removed by the reaction with OH, with vastly different reaction rates (Baker et al., 2011a, 2016). The timespan of NMHC removal ranges from regional to intercontinental transport time scales (Baker et al., 2010; Honrath et al., 2008; Parrish et al., 2007, 1992).

2. Experimental and applied methods

The CARIBIC measurements have been ongoing since 2005 and have become part of the European Research Infrastructure IAGOS (www.iagos.org). CARIBIC involves the monthly deployment of an automated measurement container on board of a specially equipped Lufthansa passenger aircraft (Airbus A340-600) during flights between Frankfurt, Germany and various destinations around the world (Brenninkmeijer et al., 2007). The cruise altitude of 10–12 km enables regular investigation of the upper troposphere and lowermost stratosphere (UTLS) on a near-global scale. In March and October 2009 and from November 2010 to March 2011 destinations were Cape Town and Johannesburg (Fig. 1 and Table 5 in the supplement). The dataset is biased in seasonality since no CARIBIC flights to Africa are available in boreal spring or summer (April to August).

The fully automated CARIBIC container comprises 15 measurement systems and carries out in-situ trace gas and aerosol particle measurements, remote sensing, and collects aerosol particle and whole air samples (Brenninkmeijer et al., 2007). The in-situ measurements provide the largest data density, whereas the air samples allow for detailed post flight analyses of a much larger number of trace gas species.

2.1. Air samples

Whole-air samples (WAS) are collected in two different collecting devices using a common metal bellows pumping system. The first one (TRAC) consists of 28 glass flasks (2.7 L volume) and the second (HIRES) of 88 stainless steel flasks (1.2 L volume) which are sequentially flushed and pressurized to 4.5 bar. The filling time

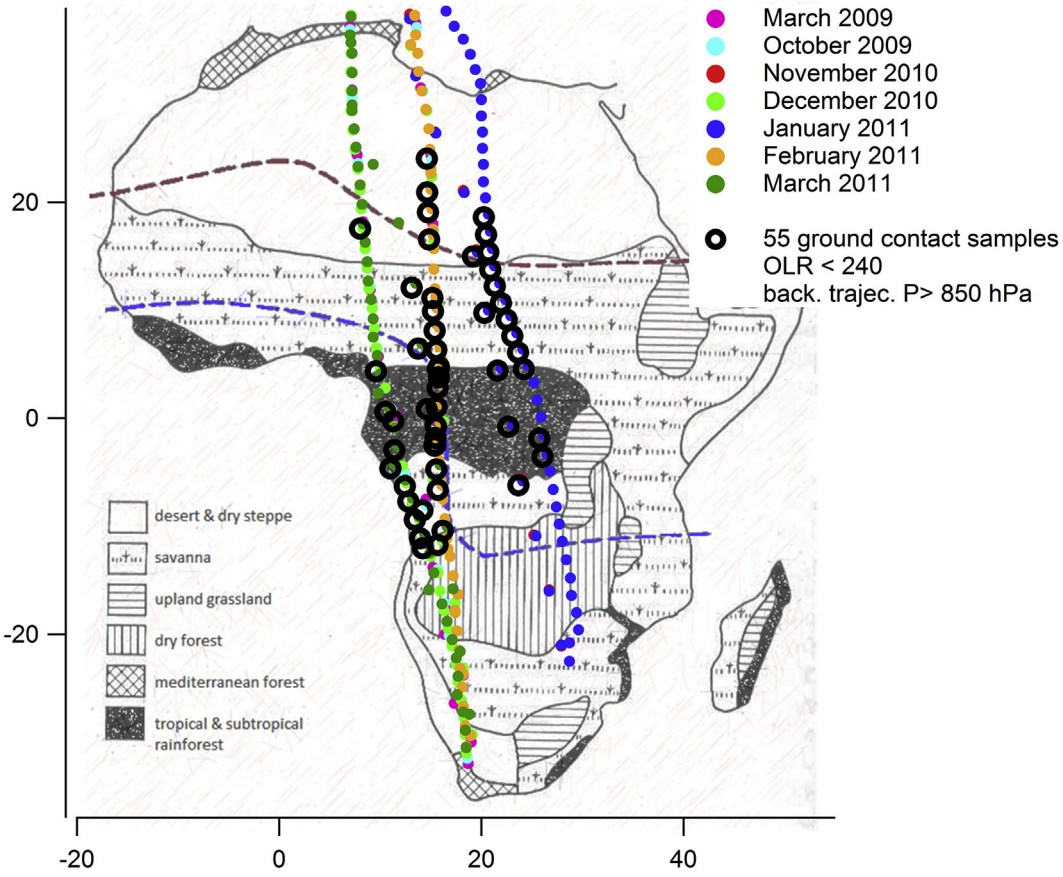

Fig. 1. An overview of flights traversing Africa. Circles indicate the sampling locations for NMHC. The dashed lines indicate the ITCZ in August (red) and January (blue) based on (Goudie, 1996). The thick circles mark the samples representing boundary layer air, according to backward trajectories and convection based on OLR satellite data (see Section 2.4). Vegetation types are adapted from Murdock (1959). (For interpretation of the references to colour in this figure legend, the reader is referred to the web version of this article.)

is altitude/pressure dependent and takes between 30 and 90 s, which corresponds to a flight distance of 7 km–22 km at a flight speed of 240 m s^{-1} (Baker et al., 2008; Schuck et al., 2009).

The whole-air samples are analyzed in Mainz, Germany for greenhouse gases (carbon dioxide CO_2, methane CH_4, nitrous oxide N_2O, and sulfur hexafluoride SF_6) and C_2 to C_8 NMHC, usually within 2 weeks after the flight, and subsequently for halocarbons at UEA in Norwich, UK usually within 8 weeks. Greenhouse gases and NMHC are analyzed in both sampling devices TRAC (6 units available of which 2 are in the container during flight) and HIRES (one unit only), while for logistical reasons halocarbons are analyzed in samples from TRAC only. Greenhouse gases are measured using gas chromatography and an electron capture detector/flame ionization detector (GC-ECD/FID) described in Schuck et al., 2009; NMHC and methyl chloride are measured using a GC-FID system (Baker et al., 2010) and the halocarbons are measured using several GC-MS systems as detailed in Leedham Elvidge et al. (2015) and Wisher et al. (2014). In our analysis we focus on a subset of measured halocarbons: methyl chloride, tetrachloroethylene, dichloromethane, chloroform and bromoform (CH_3Cl, C_2Cl_4, CH_2Cl_2, $CHCl_3$ and $CHBr_3$), which were measured reliably during all Africa flights.

2.2. In-situ measurements

CO, CH_4, H_2O mixing ratios and aerosol particle number concentration measurements were made in-situ. An overview of these measurements is given in Table 1. This analysis is constrained to the aforementioned compounds, since they were measured in almost every flight between March 2009 and March 2011 during the flights to South Africa and do not show a strong inter flight variability (NO/NO_y) or strong seasonality (CO_2).

2.3. Meteorological data and tropospheric air masses

We focussed our analysis on tropospheric in-situ measurements and WAS between 35° N and 35° S. Stratospherically influenced WAS were excluded on the basis of N_2O, a compound that shows a sharp gradient across the tropopause. It is long-lived and well mixed in the troposphere and photochemically destroyed in the stratosphere (Assonov et al., 2013; Umezawa et al., 2014). We identified the stratospheric air samples by comparing the measured N_2O with the long-term trend measured at Mauna Loa (Ishijima et al., 2010). Using the N_2O stratospheric tracer method we exclude 8% of NMHC samples (TRAC & HIRES) and 7% of halocarbon samples (TRAC) as stratospherically influenced. Moreover, based on the N_2O measurements a threshold O_3 tropopause was derived for the in-situ data, for which no N_2O data are available (N_2O being only measured for WAS). The O_3 mixing ratio corresponding to the WAS was plotted and the N_2O stratospheric tracer identification was used to find a conservative limit, being 85 ppb O_3 (supplement, Fig. 10), so that stratospherically influenced air masses were excluded. This method excluded 1.0% of CO measurements, 1.9% for CH_4, 1.2% for H_2O, 1.1% for nucleation mode particles ($N_{4\text{-}12}$) and 2.4% for accumulation mode particles (N_{140}). Stratospheric samples were mainly excluded between 25°S and 35°S and 25°N-35°N, where subtropical tropopause folds and/or extratropical stratospheric air can be found. Meteorological analysis is based on the ECMWF re-analyzed data determined along the flight track for each

Table 1
In-situ measured compounds, measurement techniques and references.

Compound	Measurement technique	Literature description
CO	resonance ultraviolet fluorescence	Brenninkmeijer et al., 2007 Scharffe et al., 2012
CH_4	modified Off-Axis ICOS analyzer	Dyroff et al., 2014
H_2O	chilled mirror frost-point hygrometer & photoacoustic diode-laser spectrometer	Dyroff et al., 2015
particle number concentration N_{140}	condensation particle counter	Hermann and Wiedensohler (2001)
particle number concentration $N_{4\text{-}12}$	optical particle size spectrometer	Hermann (2003); Hermann et al. (2016)

individual sample (van Velthoven, 2016). Meteorological fields such as wind, temperature and specific humidity are retrieved at a $1^\circ \times 1^\circ$ horizontal resolution at time intervals of 6 h, and they are interpolated to flight track locations at 1 min time steps. The KNMI TRAJKS model calculates 5 day backward trajectories along the flight track at 3 min intervals (Scheele et al., 1996) and for WAS 8 day backward trajectories are calculated based for the sampling time interval at 10s time steps. For each flight the interpolated outgoing longwave radiation (OLR) daily mean values provided by the NOAA earth system research laboratory physical science division, Boulder, Colorado, USA (www.esrl.noaa.gov/psd/), were downloaded for a 10 day time interval, centered on the flight day and the mean OLR values superimposed on a map of the flight route to assess cloud distributions.

2.4. Air masses with boundary layer contact

Emission ratios and photochemical processes were studied using a subset of tropospheric samples representing air masses that had undergone recent contact with the PBL over the African continent (<5 days). The occurrence of PBL contact was determined either by meteorological analysis using backward trajectory analysis, or by verifying proximity to major convective systems, using OLR satellite data. Air masses whose back trajectories had reached pressures of above 850 hPa within the prior five days were classified as PBL influenced ($n = 35$). Cases of strong convection ($n = 47$), when back trajectory analysis is unreliable (Andreae et al., 2001), were identified by OLR $\leq$ 240 W m^{-2} (Nguyen and Duvel, 2008).

If either criterion was met (both criteria met 50% of cases), backward trajectory pressure above 850 hPa or OLR values $\leq$ 240 Wm^{-2}, air sampled was presumed to have had PBL contact. This created a subset of $n = 55$ samples. The distribution of these samples is displayed in Fig. 1.

2.5. Source apportionment methods

Sources of the sampled trace gases were characterized with the help of the source apportionment positive matrix factorization (PMF) method, specifically using the US EPA PMF 5.0 software (U.S. EPA, 2014). It assumes that measured mixing ratios at the receptor site, in this case the aircraft, are linear combinations of contributions from different sources (Li et al., 2015; Paatero et al., 2014; Paatero and Tapper, 1994). Based on the uncertainties within the observed mixing ratios, the PMF solution minimizes the objective function Q (U.S. EPA, 2014) with u_{ij} = uncertainty estimate for the source j measured in the sample i.

$$Q = \sum_{i=1}^{m} \sum_{j=1}^{n} \left[\frac{X_{ij} - \sum_{k=1}^{p} g_{ik} f_{kj}}{u_{ij}} \right]^2 \quad (1)$$

The best PMF solution should make the Q value equal to $Q_{theoretical}$, which can be calculated according to equation (2), where i = number of samples, j = number of species, p = number of sources.

$$Q_{theoretical} = i \times j - p \times (i + j) \quad (2)$$

In PMF analyses there is an inherent uncertainty due to random errors and a possible rotational ambiguity, i.e. many possible solutions can equivalently represent the measured data. The EPA PMF software uses three methods for estimating this uncertainty which are: classical bootstrap, displacement of factor elements, and bootstrap enhanced by displacement of factor elements (Paatero et al., 2014). We used these methods to evaluate the results calculated with the PMF software. How these methods work is described in Brown et al. (2015). The PMF analysis has the advantage that it is entirely based on the measured mixing ratios and their uncertainty, and does not need source emission ratios as input. However, emission sources derived from the PMF analysis need to be compared to known source emission ratios to ascertain their identity.

3. Results and discussion

The effects of strong convective transport to flight altitude near the ITCZ, mixing of aged/background and fresh/polluted air, and the hemispheric gradient can be readily gleaned from the data. These features are discussed in the flight overview Section 3.1. The various sources of the trace gases are differentiated using NMHC in the PMF model and NMHC/CO emission ratios in Section 3.2. In the last Section 3.3, the NMHC-ratios are exploited to examine oxidation pathways and O_3 formation.

3.1. Flight overview

The latitudinal profiles over Africa of the in-situ measured trace gases (CO, H_2O, and CH_4) and aerosol particles are given in Fig. 2. The entire dataset (boreal fall and winter, Table 5, supplement) has been plotted as a whole since little latitudinal differences between the single flights are present, although the burning season migrates from the SH to the NH between September and March (Galanter et al., 2000). CO, H_2O, CH_4 and freshly formed particles (nucleation mode) consistently show maximum mixing ratios and concentrations around the equator.

The peak median CO mixing ratios (close to 150 ppb) near the equator are caused by the combination of strong surface sources and effective convective transport. CO does not show a pronounced interhemispheric gradient at this altitude (compared to CH_4) since its lifetime is shorter and convection associated with the ITCZ serves to mix air into both hemispheres in the cloud outflow region (e.g. Williams et al., 2002).

The maximum in median mixing ratio of CH_4 coincides with that of CO. The longer lifetime of CH_4 leads to a clear NH/SH gradient at cruise altitude, in contrast to shorter lived CO, while a larger relative variability for CH_4 is generated by highly variable surface sources and interhemispheric mixing. The latitudinal pattern of CH_4 mixing ratios and different sources of CH_4 in Africa, such as biomass burning and wetland emissions have already been discussed in detail by Schuck et al. (2012).

The maximum of the median H_2O mixing ratios is shifted south

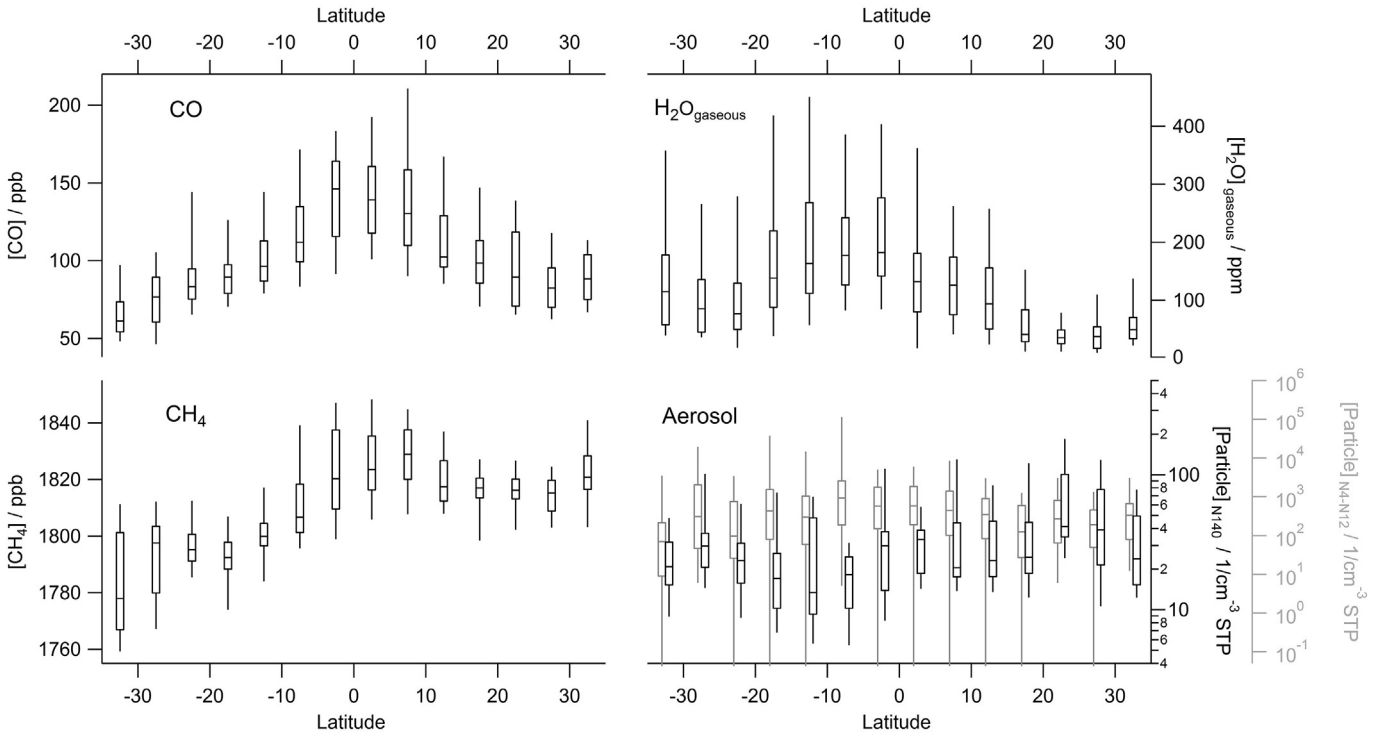

Fig. 2. Box and whiskers plot of CO, CH_4, H_2O and aerosol tropospheric data for all African transect flights. Latitudinal bins are 5° wide. Data for ascent and descent of the aircraft were removed. The boxes for CO, CH_4, H_2O and aerosols are made of more than 930, 550, 608, 600 and 448 data points, respectively. The horizontal line represents the median, the box represents the upper and lower quartile, and the whisker represents the 0.05 to 0.95 percentile. For clarity the bins in the aerosol plot have been offset by ±0.5°.

compared to CO and CH_4. H_2O is a good tracer for recent vertical transport and therefore marks the ITCZ in the UT, which over Africa is located south of the equator during boreal winter (Waliser and Gautier, 1993). North of 17.5 °N very low mixing ratios and a low variability were found, caused by the dry descending air that is characteristic of the northern part of the Hadley cell. A high variability in gaseous H_2O south of 25 °S is notable in the data covering different months. This variability is also obvious in the OLR data (Supplement, Fig. 13).

Finally Fig. 2 shows the aerosol particle number concentrations for the nucleation mode (4 nm ≤ diameter ≤ 12 nm, $N_{4\text{-}12}$) and the accumulation mode (140 nm ≤ diameter ≤ 1 050 nm, N_{140}). The nucleation mode particles are most abundant between 10°N and 20°S, similar to the H_2O data, indicating that deep convective outflow in the UT is responsible for the observed frequent new particle formation (Heintzenberg et al., 2011, 2003). Fig. 2 also presents the first ever measured UT accumulation mode particle numbers over Africa. N_{140} shows, in contrast to $N_{4\text{-}12}$, a minimum in the tropics and higher values towards higher latitudes. These contrasting gradients of N_{140} are caused by the removal of these larger particles in clouds by nucleation and impaction scavenging, again indicating the position of deep convective clouds and thus the ITCZ (Liu and Zipser, 2005).

The qualitative summary of the latitudinal profiles is therefore that H_2O is the best tracer for the ITCZ, whereas CO and CH_4 are prominent at cruise altitude where surface sources are active. Fig. 2 (CH_4 and CO) also reminds us that Africas largest land masses, and hence trace gas sources for the discussed species, are north of the equator.

Although air sampling provides a lower data density along the flight tracks, similar patterns as discussed above for CO, CH_4, H_2O and aerosol particles ($N_{4\text{-}12}$) are discernible for ethane, ethyne, propane and benzene in Fig. 3. The decrease in relative variability (box and whisker length) from benzene > propane ≈ ethyne > ethane is inversely proportional to the lifetime of these NMHC (Table 2). This relationship is the result of both the mixing of freshly polluted air and aged background air, and photochemical processing between source and measurement. The two processes, dilution and photochemistry, act in concert yielding the same effect and, only when the sources are very close does the relationship breakdown.

The halocarbon overview (Fig. 4) shows that C_2Cl_4, CH_2Cl_2, and $CHCl_3$, have, compared to the NMHC, a more pronounced NH/SH gradient, with generally higher mixing ratios at the more northerly latitudes. The latitudinal gradient is strongest for CH_2Cl_2 and decreases via C_2Cl_4 to $CHCl_3$ with $CHBr_3$ barely exhibiting a gradient. The relative differences in NH/SH gradients correspond inversely to the atmospheric lifetimes of the species (Table 2) and the predominant NH source locations. To investigate the source locations of halocarbons further, eight day back trajectories were examined (Fig. 11, supplement) revealing mainly eastwards transport with convection above the African continent, the Atlantic and South America. Sources of CH_2Cl_2 and C_2Cl_4 are primarily industrial (Leedham Elvidge et al., 2015; Simpson, 2004) and therefore predominantly found in the NH. For $CHCl_3$ and $CHBr_3$, besides minor industrial sources, strong natural oceanic and terrestrial sources are known (Gebhardt et al., 2008; Laturnus et al., 2002; Leedham et al., 2013; Real et al., 2010). $CHBr_3$, the compound with the shortest lifetime, has a convection dominated distribution pattern, with elevated mixing ratios between 10°N and 10°S. A difference between the halocarbons and the NMHC is in the type and distribution of their sources. In general, NMHC have common sources associated with fossil fuel use with well-defined emission ratios for the different NMHC. Halocarbons on the other hand can have quite variable emission strengths dependent on the specific sources. The overview of CH_3Cl (methyl chloride) for the Africa flights of the CARIBIC-observatory was recently discussed by Umezawa et al. (2014), (supplement Fig. 12). The mixing ratios of CH_3Cl increase

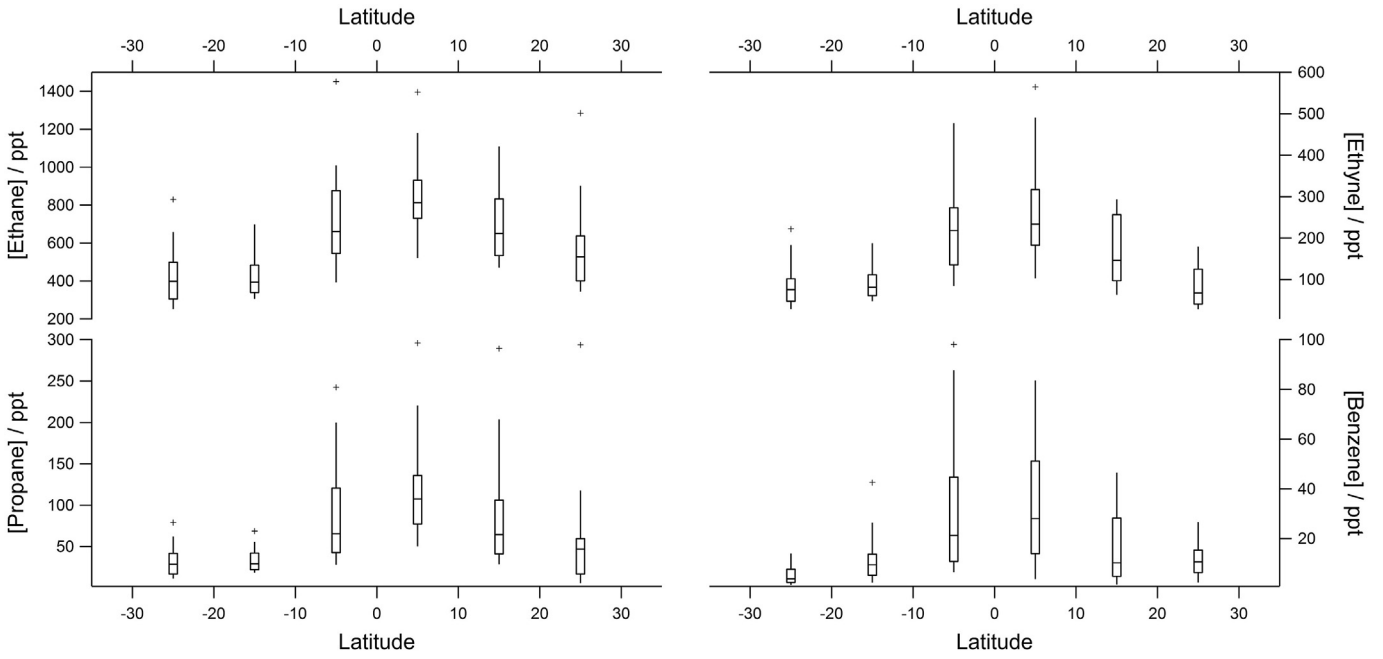

Fig. 3. A box and whiskers plot (see Fig. 2 description) of ethane, ethyne, propane and benzene as a function of latitude during the 13 *trans*-African flights. Latitudinal bins are 10° wide. Each box comprises datasets of n ≥ 25, except benzene latitude bin 25° where n = 20. Data from March 2009 to March 2011 was used (9 flights sampled in glass flasks (TRAC) and 4 flights in metal flasks (HIRES), see Section 2.1). Outliers are shown as crosses and are more than 1.5 times the box width off the median.

Table 2
Atmospheric lifetimes and rates of reaction for oxidation with OH- and Cl-radicals for the NMHC and halocarbons analyzed in this study. X = no data available.

Compound		Mean atmospheric lifetime/days	k OH at 298 K
Ethane[a]	C_2H_6	50	2.40×10^{-13}
Propane[a]	C_3H_8	12.5	1.10×10^{-12}
n-butane[a]	n-C_3H_{10}	5	2.35×10^{-12}
i-butane[a]	i-C_3H_{10}	6	3.80×10^{-12}
Ethyne[a]	C_2H_2	12	7.80×10^{-13}
Benzene[a]	C_6H_6	9.4	1.20×10^{-12}
Toluene[a]	C_7H_8	1.9	5.60×10^{-12}
methyl chloride[b]	CH_3Cl	548	3.60×10^{-14}
Tetrachloroethylene[b]	C_2Cl_4	90	1.52×10^{-13}
Dichloromethane[b]	CH_2Cl_2	144	1.00×10^{-13}
Chloroform[b]	$CHCl_3$	149	1.00×10^{-13}
Bromoform[b]	$CHBr_3$	24	1.20×10^{-13}

[a] (Atkinson, 2003).
[b] (Montzka and Reimann, 2010).

from the NH towards the equator and stay high going further south, showing a strong influence of CH_3Cl sources in Africa which are BB and non-combustion sources, mainly vegetation emissions (Umezawa et al., 2014).

3.2. Trace gas sources

To investigate the sources of the trace gases in the air masses encountered, two different approaches are employed. The first is a source apportionment approach using PMF; the second exploits enhancement ratios of NMHC relative to CO. For the PMF approach, the whole tropospheric dataset of NMHC (n = 230) was used (Section 2.3) excluding species that were below the detection limit more than 25% of the time (e.g. i-butane, toluene). The in-situ measured compounds were not part of the dataset since the correlation between CO, CH_4, H_2O and particles was tested with the source categories resulting from the PMF analysis. The halocarbons are part of a much smaller dataset (n = 91), because they were measured from the TRAC-samplers only (Section 2.1). When halocarbons were included swaps in the displacement (an error estimation within PMF) occurred for all runs, showing that the solutions of the PMF analysis were not well defined. We therefore excluded the halocarbons to have the dataset of n = 230 measurements for the NMHC. The eligible data for PMF included: ethyne, ethane, propane, n-butane and benzene. Secondly, the enhancement ratios approach was applied to investigate BB emissions. For this analysis the dataset was filtered to include only the aforementioned samples with PBL contact (n = 55) to calculate the enhancement ratios (Section 2.4).

3.2.1. PMF for source apportionment

PMF is a multivariate analysis method that decomposes the matrix of measured sample concentrations into two matrices of source profiles, the emission pattern of each source, and source contributions, the relative amount each profile has. For this statistical method no source emission profiles are needed as input. The calculation of both source profiles and contributions is based on the matrix of measured compounds only. To use this method the PMF

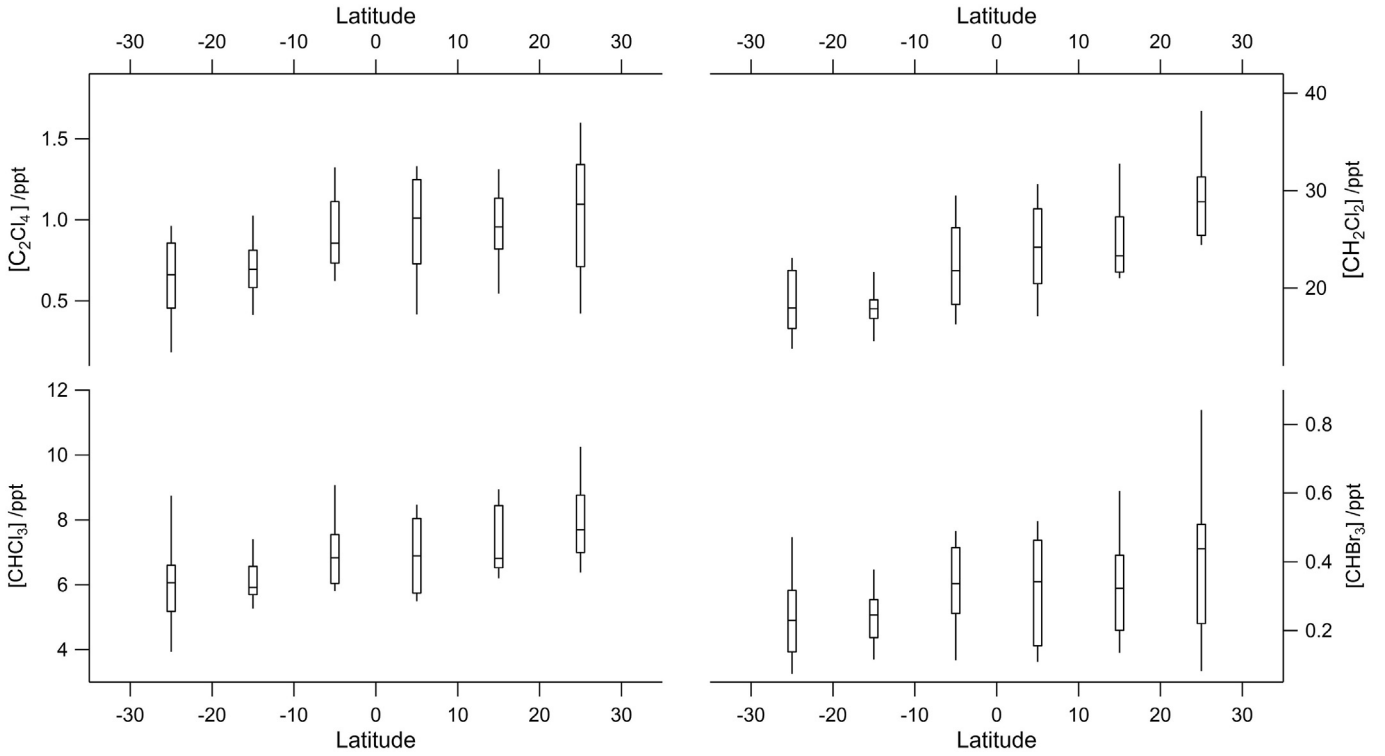

Fig. 4. Box-Plot (See Fig. 2 description) of C_2Cl_4, CH_2Cl_2, $CHCl_3$ and $CHBr_3$ during the flights to Africa. Latitudinal bins are 10° wide and each box comprises a dataset of n ≥ 15 except $CHBr_3$ latitude bin −25 where n = 12, the sample numbers are smaller than NMHC, since the halocarbon analysis is done only for the glass flask sampler (TRAC).

5.0 software (U.S. EPA, 2014) was utilized, which uses the sample concentration and user provided uncertainty of the sample data to weight the individual data points in the data matrix. PMF is used as a tool to identify the sources of trace gases such as NMHC, and their relative impact at a given location. This tool has been applied previously on data collected from surface sites, close to the sources of different VOCs (Buzcu and Fraser, 2006; Shao et al., 2016; Song et al., 2007), and on datasets containing several VOC groups. Here we extend the use of this method to NMHC samples measured in the UT above Africa far from the sources. Therefore our dataset is biased to the few longer lived compounds that are measured above the detection limit in more than 25% of the measurements. This precludes differentiation of some closely related sources, such as particular fuels like LPG or natural gas, as such fine distinctions require multiple shorter lived compounds. The evaluation of the PMF results in this manuscript is therefore focused on the main general source characteristic, which is accessible with the measured longer lived NMHC mixing ratio matrix. To evaluate the PMF results the source profiles resulting from the analysis were compared to literature values and the resulting source contributions were compared to the in-situ data measured during the *trans*-Africa flights. The uncertainty matrix of the data was calculated by the PMF software using the concentration as well as the methods detection limit (MDL) and the species specific measurement uncertainty (Error Fraction), both derived from Baker et al. (2010) for the applied analytical method.

The limit of detection was 1 ppt for all compounds except benzene where we used the detection limit of 3 ppt. The uncertainty used in the model was 0.9%, 0.2% 0.8% 0.3%, 0.4% and 2.3% for ethyne, ethane, propane, n-butane and benzene respectively and all results should be considered with this uncertainty in mind. To investigate the suitable number of sources we modeled two to four sources. The PMF software calculated chemically unrealistic single compound sources for five or more sources, due to the fact that only five compounds were used for the calculation. The three sources solution was deemed to be most representative based on the resulting source profiles and the statistical error estimation within the PMF software. The observed and predicted scatter plots for the three sources solution showed a good correlation for the different species close to the 1:1 line. The residuals of the three sources solution were normally distributed within the −3 to 3 sigma interval and the calculated source profiles were comparable with source profiles from literature. The error estimation also favored the three source solution. The first error estimate displacement of factor elements showed no mismapping, which means that the solution is well defined for all tested source numbers, but the second error estimate the classical bootstrapp had displacements for the two or four source solutions tested. This displacement in bootstrap is a sign that either too many factors were used (four sources) or that factors with a low reproducibility occur infrequently in the data (Brown et al., 2015). If two sources are used although in reality there are three sources, the dataset produces mixed sources which reduce the reproducibility of the dataset. For

$$uncertainty = \sqrt{(Error\ \ Fraction\ \ x\ \ concentration)^2 + \ (0.5\ x\ \ MDL)^2} \quad (3)$$

the three sources all bootstrap factors were mapped, which shows that from a statistical point of view the three sources solution is the most realistic one, which in addition to the comparability to literature emission sources is the reason we used the three source solution for the discussion.

To attribute the calculated PMF sources displayed in Fig. 5 to probable emissions, the source profiles calculated by the PMF model were compared to emission profiles from literature. Since all NMHC have the same removal pathway (namely OH) the calculated sources are comparable to emission sources on the ground despite the calculated sources being based on measurements in the free troposphere far away from the surface sources. The first source, termed "fossil fuel", was attributed to the emission of fossil fuels/natural gas because it mainly consists of saturated alkanes (ethane, propane, n-butane) with only a minor contribution of unsaturated compounds (ethyne, benzene). Moreover, the pattern follows the abundances of the different NMHC in liquefied petroleum (LPG) with ethane > propane > n-butane. The saturated C2-C4 alkanes which are elevated in the PMF source profile are often associated with fugitive emission and combustion of natural gas or LPG (Baker et al., 2008). Since the higher alkanes C5-C8 which would indicate vehicular emissions have shorter lifetimes and are depleted below the detection limit before they arrive the sampling altitude we cannot exclude them from the source emissions (Baker et al., 2008; Chan and Wang, 2000; Mühle, 2002). Therefore we call the source associated with the PMF source profile fossil fuels which should include both fugitive emission and combustion processes of natural gas/LPG and vehicular fuels. The second source calculated, labeled "biomass burning" (BB), was attributed to the NMHC emission during burning of biomass. The comparatively high mixing ratios of benzene and ethyne, both unsaturated compounds, are known components of biomass burning of grassland or tropical forest (Andreae and Merlet, 2001). In the BB source, the abundance decreases in the order ethane (195 ppt), ethyne (136 ppt), benzene (15 ppt) and propane (13 ppt) which is comparable to the decrease of emission factors, related to the mass of biomass burned, reported for savanna burning from two literature studies (Akagi et al., 2011; Andreae and Merlet, 2001), of 0.66, 0.24, 0.20 and 0.10 g $kg^{-1}_{(burned\ biomass)}$ and 0.32, 0.29, 0.23 and 0.09 g $kg^{-1}_{(burned\ biomass)}$, respectively. The biomass burning source of NMHC is discussed in the next section in more detail. The third source calculated, "background", was so-named as the mixing ratios of the NMHC for this source were proportional to their atmospheric lifetimes (Table 2). We contend that any mixture of NMHC subjected to OH chemistry for a prolonged period will tend towards this condition, as the longer lived species persist over the shorter lived ones. The original source signature thus is lost with long processing times. The "background" source shows ethane (lifetime 50 days) as the dominant component with a strong decrease to propane (12.5 days) and ethyne (12 days), with no n-butane (5 days) or benzene (9.4 days). Keeping the detection limit and the uncertainty in mind both compounds could be still in "background" air, but their mixing ratios are too small to be resolved by the PMF model. It is interesting that the PMF analysis revealed an air mass classification of background air for the tropics as a study for the mid-latitudes and subtropics using the different statistical approach of cluster analysis for CARIBIC aerosol particle data also found a cluster of background air in the free troposphere (Köppe et al., 2009).

Comparing the source contributions to the ethane mixing ratio it is clear that ethane mixing ratios are predominantly determined by "background" air values, followed by "BB" and "fossil fuel". Ethyne and benzene mixing ratios are dominated by the "BB" source. Propane and n-butane have their main source in "fossil fuel".

In addition to the literature comparison above, we compare the source contributions of the three sources with the in-situ measurements of CO, H_2O, CH_4 and nucleation and accumulation mode particles. For this comparison we integrated the in-situ measured data over the sampling period resulting in 160 samples for CO, 141 samples for H_2O, 175 samples for CH_4, 117 samples for nucleation mode particles $N_{4\text{-}12}$ and 76 samples for accumulation mode particles N_{140}. The correlation of the source contributions for the three sources from the PMF-model and the in-situ species were tested using a *t*-test and F-test, both at a significance level $\alpha = 0.05$. The results of the test for each in-situ compound can be found in the supplement material. The source contribution correlation with CO (Fig. 6) and CH_4 showed decreasing correlation coefficients r^2 in the sequence from BB, fossil fuel to background source from 0.43 to 0.16 and 0.01 and from 0.25 to 0.17 and 0.02, respectively. For both trace gases a significant correlation was found for the BB and fossil fuel sources with both F-and t-tests, and for both gases no correlation was found for the "background" source. The significant correlation between the two in-situ gases, CO and CH_4, and the "BB" or "fossil fuel" source contribution is an indication that those sources are determined by emissions from the surface and therefore the correlation also supports the PMF results for the source

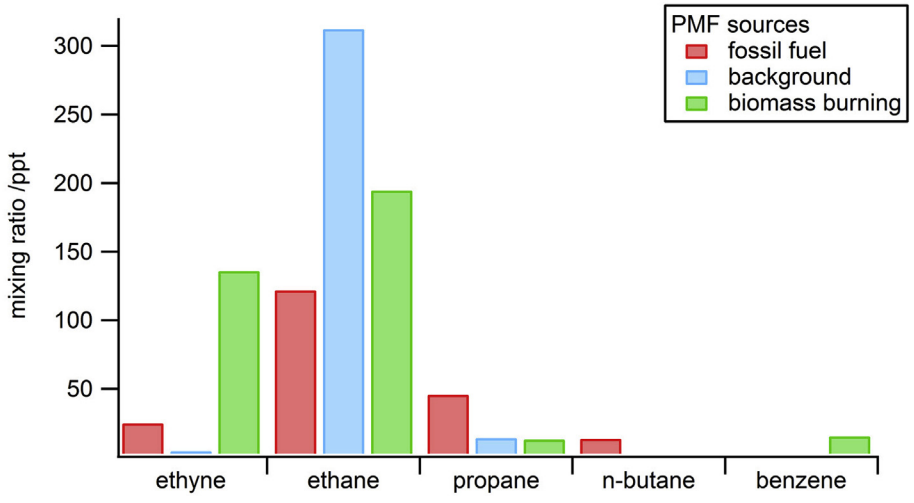

Fig. 5. PMF s calculated using PMF 5.0 software for the samples between 35°N and 35°S during the Africa flights (see Section 2.3 for details).

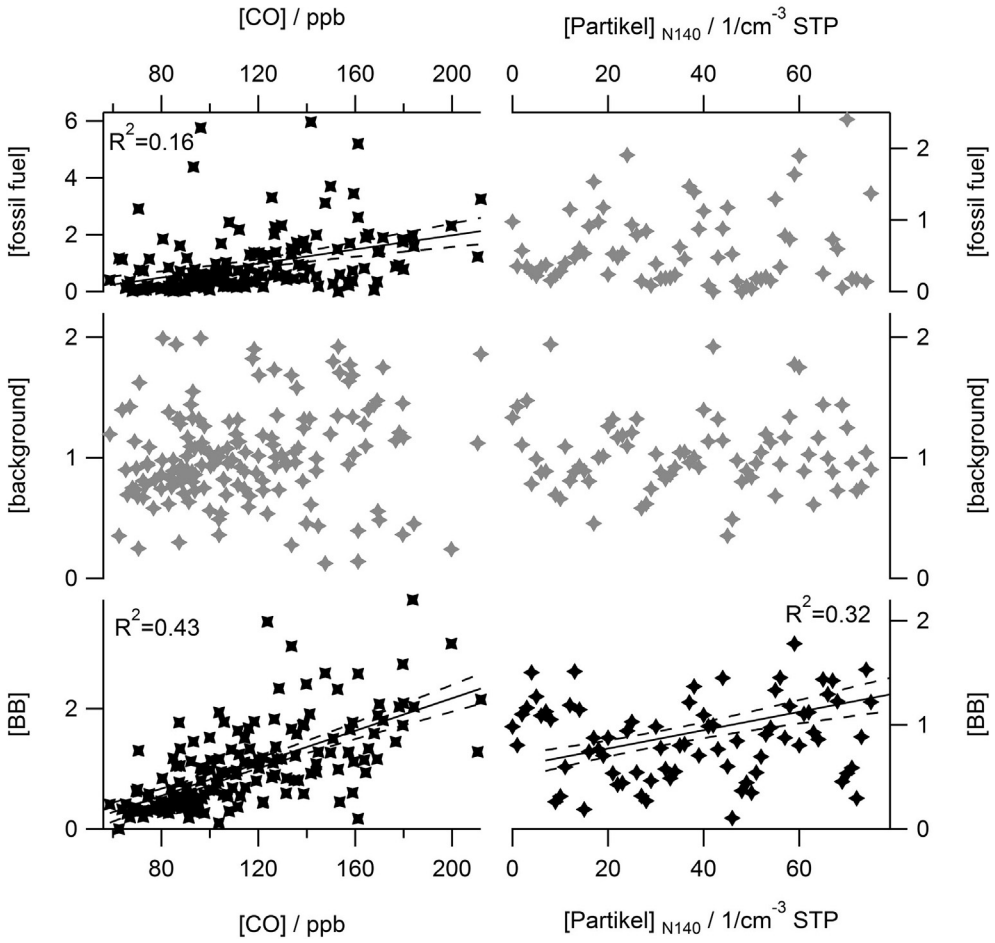

Fig. 6. Correlation between the factor contribution of the PMF factors fossil fuel, background and biomass burning versus the CO mixing ratios and versus particle numbers for the accumulation mode calculated or measured for each CARIBIC sample. The lines show the calculated correlation and the 95% confidence interval of the slope. The whole tropospheric dataset is shown for the PMF analysis (n = 230).

apportionment. The good correlation for the "BB" source contribution is expected since both CO and CH_4 are emitted during incomplete combustion of biomass (Andreae and Merlet, 2001; Khalil and Rasmussen, 1990; Kirschke et al., 2013). The correlation for the fossil fuel source contribution and CH_4 is also expected since CH_4 is associated with the exploitation of gas, oil and coal (Kirschke et al., 2013). The correlation of the fossil fuel source contribution with CO shows that the calculated PMF source named fossil fuel also contains emissions from incomplete combustion of fossil fuel (Gros et al., 1999; Khalil and Rasmussen, 1990). The lack of correlation between both in-situ gases and the background source contribution is an indication that the "background" is not related to surface sources. It can be concluded that in the upper troposphere region the air is well aged so that all ground source influence has been lost. The accumulation mode particle data (N_{140}) correlate significantly (t- and F-test) with the BB source profile ($r^2 = 0.32$) (Fig. 6), indicating that the accumulation mode particles measured are at least partly formed during BB, which is known source of airborne particles above Africa (Capes et al., 2008; Johnson et al., 2008; Matsuki et al., 2010) and that this information is preserved during transport and aging of the air mass to the sampling altitude. The particle data are not correlated with fossil fuel and background PMF profiles. The H_2O data and the data of the nucleation mode particles ($N_{4\text{-}12}$) show no correlation with the source contribution of any source profile calculated with the PMF analysis. That both these in-situ compounds show similar behavior here and in the overview indicates that the measurements were taken in the outflow of deep convective clouds, which transport water to the UT, and where new particle formation is expected, independent of sources of precursor gases (BB or fossil fuel).

3.2.2. Enhancement ratios and biomass burning

To investigate the sources of the trace gases from Africa, the boundary layer influenced dataset (Section 2.3, Fig. 1) was used, with the additional two compounds toluene and CH_3Cl. Toluene is included in the PBL dataset, since it is measured above the detection limit in 35% of the cases compared to the whole tropospheric dataset (<25%). CH_3Cl is now included since the correlation analysis can be done even if this compound has a relatively high analytical uncertainty (Umezawa et al., 2014). To determine enhancement ratios ($\Delta X/\Delta CO = (X_{sample}-X_{background})/(CO_{sample}-CO_{background})$), background values are necessary. The NMHC background calculated from the PMF source "background" was therefore used for ethyne, ethane, propane, and benzene. Toluene, which has a shorter lifetime than n-butane, was assumed to be zero in background air, which is in line with the PMF result. The CH_3Cl background was assumed to be 550 ppt (Umezawa et al., 2014). For the CO background 70 ppb was assumed which is the mean in CO between 35°S and 25°S in the overview, where convection and sources are low compared to air influenced from the boundary layer. ΔNMHC/ΔCO was then derived from NMHC-CO-scatter plots which are shown in Fig. 7. All NMHC (ethane, propane, ethyne, benzene and toluene)

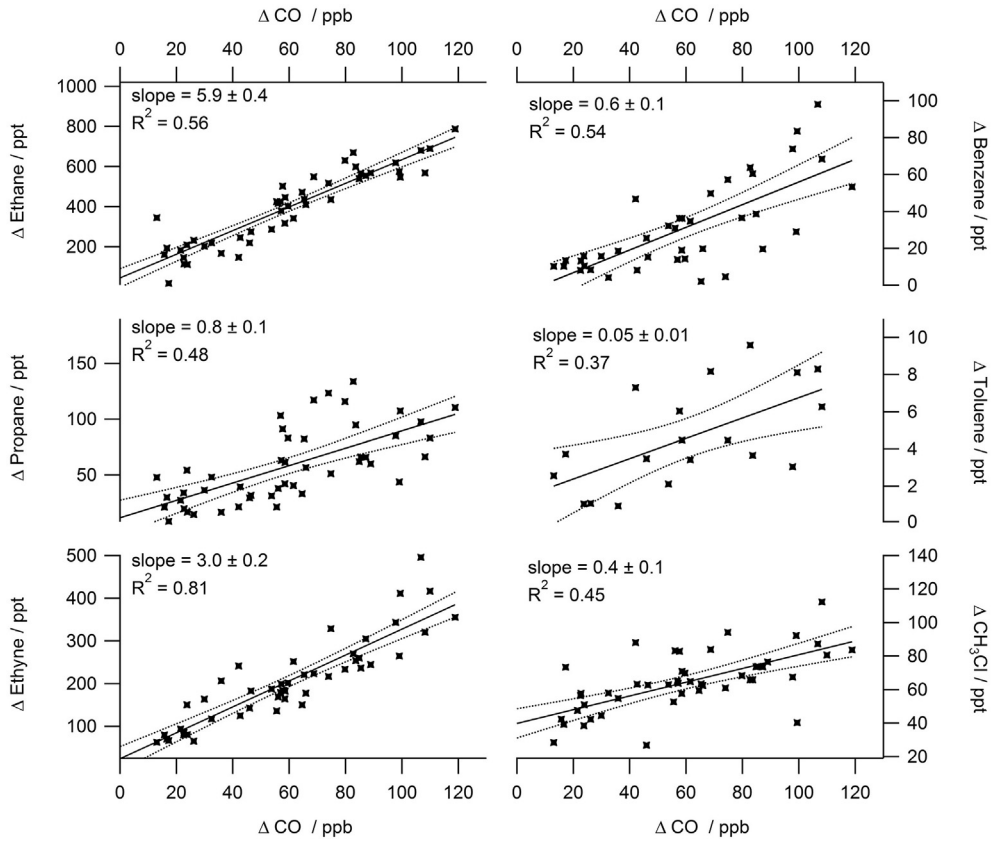

Fig. 7. Correlation plots of enhancement ratios of NMHC and halocarbons vs. CO for samples which showed recent contact to the PBL (n = 55) (see Section 2.4). Slopes of the correlation have units of pptv NMHC/ppbv CO and the uncertainty represents the 95% confidence interval of the slope.

and CH_3Cl, show a significant correlation with CO ($R^2 > 0.37$). Ethyne and benzene are well correlated with CO ($R^2 = 0.81$ and $R^2 = 0.54$, respectively) due to their shared combustion sources for example BB (Baker et al., 2011b). CH_3Cl is also emitted by BB, but the correlation nevertheless is somewhat weaker ($R^2 = 0.44$) than for the unsaturated NMHC, which could be explained by a relative small enhancement in CH_3Cl due to BB emissions compared to a large background especially in the tropics (Khalil and Rasmussen, 1999). However, even gases with other, non-combustion sources, such as ethane and propane, show strong correlations with CO ($R^2 = 0.86$ and $R^2 = 0.50$, respectively) which can be attributed to co-located sources and well mixed air masses during transport from the ground. The weakest correlation with CO is seen for toluene ($R^2 = 0.37$), again a compound with a significantly shorter lifetime than CO.

The enhancement ratios between ethane, propane, ethyne, benzene, toluene, CH_3Cl and CO were compared to enhancement ratios calculated for single air samples during a flight from Windhoek to Munich, conducted within the first phase of the CARIBIC project called CARIBIC1 in a BB plume in 2000 (Mühle, 2002), and to ratios measured during BB plume events during the TRACE-A campaign 1993 in Southern Africa (Mauzerall et al., 1998), see Table 3. The calculated enhancement ratios for ethane, propane and CH_3Cl are in the medium range of the enhancement ratios previously reported in recent and aged BB plumes (Mauzerall et al., 1998; Mühle, 2002), whilst the enhancement ratios of the unsaturated compounds ethyne, benzene and toluene are in the lower part of the enhancement ratio range given in the literature. In typical BB investigations the ER is calculated from measurements which are clearly inside a BB plume for the sample values, and outside the plume for background values. In our study, the enhancement ratios of NMHC and CH_3Cl from Africa were calculated for samples which had had recent (<5 days) contact to the PBL (Section 2.3), regardless if they were in a BB plume or not. The good agreement of these measurements and literature values in BB plumes show that the samples measured during the 13 *trans*-Africa flights are mainly influenced by BB. This result is consistent with satellite data of active fires during a ten day period before and during the flight days by MODIS (Giglio et al., 2003). The low ratios of unsaturated NMHC (Δbenzene/ΔCO, Δtoluene/ΔCO and Δethyne/ΔCO) which are emitted by BB indicate that the air masses we investigate are aged BB plumes. In a BB plume the enhancement ratios decrease and progressively disappear faster with the shorter lifetime of NMHC (Mauzerall et al., 1998). During the aging of a plume both reaction with OH and mixing with background air occur, and both reaction and mixing have the same effect in that they reduce the enhancement ratios. Thus these two effects cannot be separated. To investigate both processes separately from another more than one NMHC emission ratio is necessary (Baker et al., 2011b; Parrish et al., 2007). This analysis is described in the next Section 3.3.

To investigate the type of biomass that produced these signals we compare the calculated enhancement ratios to source emission ratios for BB of different biomass classes (Akagi et al., 2011; Andreae and Merlet, 2001). To facilitate comparison, the aircraft observed enhancement ratios were age corrected. The age correction was based on the relationship between initial enhancement ratio (ER_0) and the ratio determined from the measurement (ER_t) from equation (4) which is a well-established method to compare ground data to aircraft measurements (Baker et al., 2011b; de Gouw et al., 2001; Scheeren et al., 2003).

Table 3
Enhancement ratios for biomass burning in this study and the existing literature. Units are ppt ppb^{-1}

	BB plume	Fresh to recent BB plume	PBL contact air over Africa
	(Mühle, 2002)	(Mauzerall et al., 1998)	This study
Ethane/CO	3.4–5.1	5.2–8.2	5.9 ± 0.4
Propane/CO	0.7–1.6	0.8–3.2	0.8 ± 0.1
Ethyne/CO	2.9–3.9	2.9–4.6	3.0 ± 0.2
Benzene/CO	0.9–1.3	0.8–1.4	0.6 ± 0.1
Toluene/CO	–	0.2–0.8	0.1 ± 0.1
CH3Cl/CO	0.2–0.3	–	0.4 ± 0.1

$$ER_t = ER_0 e^{-((k_{CO}-k_A)|OH|\Delta t)} \quad (4)$$

In this equation ER_t and ER_0 are ratios of a compound A to CO in the air mass at the measurement time, and at the source, respectively, k_{CO} and k_A are the reaction rate constants of CO and compound A with OH (Table 2), $|OH|$ is the spatial and temporal average OH concentration encountered by the air parcel during transport time Δt. This method does not account for mixing with other air masses, which in reality will occur, and consequently the emission ratios estimated with this age correction provide a lower limit. The transport time Δt was estimated on the basis of the backward trajectories for each air sample provided by KNMI (van Velthoven, 2016), by counting the days since PBL contact and calculating the average for all air samples with pressures above 850 hPa within 5 days. This method results Δt = 107 h. The cases with strong convection identified by OLR measurements were not used to calculate the transport time. We used $|OH|$ of 9.3 × 10^5 molec cm^{-3} (Spivakovsky et al., 2000), which is the predicted mean OH concentration between 12°N and 12°S at 200 hPa in January. All assumptions for the age correction lead to a high uncertainty for this method, which we estimate to be around 30% (Baker et al., 2012).

The emission ratios with age correction are displayed in Table 4. The calculated emission ratio for Δethane/ΔCO is in the range of savanna and grassland burning and the emission ratio of tropical forest burning (Akagi et al., 2011; Andreae and Merlet, 2001). The age corrected emission ratio for Δpropane/ΔCO is comparable to the ratio for savanna burning from Akagi et al. (2011). The ratios for the unsaturated and aromatic compounds Δethyne/ΔCO and Δbenzene/ΔCO are low for savanna and tropical forest burning compared to both literature studies. There are two possible reasons for the lower age corrected emission ratios for the unsaturated compounds compared to the saturated; 1) mixing with background air, which is discussed in the next section and 2) the lower ratio could mean that the mean real transport time is longer than the one used in the age correction, since during the longer transport time the ratio would decrease more by reactions with OH and conversely the age corrected ratio would be higher and therefore fit literature values more closely. The calculated Δtoluene/ΔCO and ΔCH_3Cl/ΔCO enhancement ratios lie between savanna and tropical forest for both literature studies. All age corrected ratios, except ΔCH_3Cl/ΔCO, are clearly smaller than the biofuel burning ratio from Andreae and Merlet (2001), therefore the burning of biofuel plays only a subordinate role as source for the NMHC traces in the UT above Africa. Comparison of age corrected emission ratios with the literature values for emission ratios should be made with caution due to both the uncertainties inherent in the age correction and to high variability in emission ratios from source measurements. Nevertheless, the age corrected emission ratios calculated here point towards the burning of savanna/grassland and tropical forest as a major source for NMHC in the UT above Africa. During this time of the year (October–March), when samples were taken, the burning season in the NH moves from the northern to the southern Sahel, where woodland (19%), grassland (17%), shrubland (7%) and cropland (12%) is burned (Roberts et al., 2009).

3.3. Photochemical processes in the upper troposphere

In Section 3.1, the differences in NMHC mixing ratio variability in the ITCZ region was discussed and the effect attributed to both mixing and their different photochemical lifetimes. In general, these differences in NMHC lifetime can be used to investigate the photochemical processing of air masses. Therefore we use the ratios between two NMHC, with different chemical lifetimes, to determine the photochemical age of air, Δt, and the degree of photochemical processing in the air masses in the convective zone of the ITCZ in Africa. The utility of using NMHC ratios to study photochemical aging and the accompanying theoretical framework has been well established in the literature (Baker et al., 2011b; Helmig et al., 2008; Honrath et al., 2008; Parrish et al., 2007, 1998). Using equation (4), Δt can be derived for an air mass undergoing OH photochemistry from the ratio between two hydrocarbons, A and B, having different rates of reaction with OH, k_A and k_B, as described in equation (5).

$$\Delta t = -\frac{1}{(k_A - k_B)[OH]} ln\left(\frac{[A]_t/[B]_t}{[A]_0/[B]_0}\right) \quad (5)$$

$[A]_t/[B]_t$ is the ratio between two NMHC measured in the air mass, and $[A]_0/[B]_0$ is their emission ratio at the source. By using the ratios instead of single compounds, dilution is accounted for a hydrocarbon free background, since the dilution is expected to act

Table 4
Emission ratios for biomass burning in the existing literature and in our study using age correction for the PBL contact air samples. Units are ppt ppb^{-1}

	Age corrected	Savanna & grassland	Tropical forest	Biofuel	Savanna	Tropical forest
	This study	(Andreae and Merlet, 2001)			(Akagi et al., 2011)	
Ethane/CO	6.0 ± 0.5	4.4 ± 2.3	10.7 ± 0.6	14.3 ± 7.2	9.8 ± 6.1	7.1 ± 3.7
Propane/CO	1.1 ± 0.2	0.8 ± 0.3	0.9 ± 0.7	4.1 ± 3.1	1.0 ± 0.1	0.9 ± 0.4
Ethyne/CO	4.0 ± 0.3	4.5 ± 3.5	4.1 ± 2.0	9.7 ± 7.2	4.1 ± 1.7	5.1 ± 4.0
Benzene/CO	0.9 ± 0.1	1.2 ± 0.6	1.4 ± 0.1	8.7 ± 4.6	1.1 ± 0.5	1.5 ± 0.5
Toluene/CO	0.7 ± 0.1	0.6 ± 0.3	0.7 ± 0.2	4.3 ± 2.7	0.4 ± 0.3	0.9 ± 0.3
CH3Cl/CO	0.4 ± 0.2	0.6 ± 0.2	0.5 ± 0.3	0.4 ± 0.1	0.5 ± 0.3	0.3 ± 0.2

equally on both NMHC. On the other hand this equation is only strictly valid for the idealized situation of an isolated air mass experiencing photochemical oxidation by OH following a single pulse of emission. Therefore this approach neglects mixing with background air, which contains longer lived compounds like ethane and propane. To account for the mixing with background air, which already contains longer-lived NMHC (Parrish et al., 1992), the comparison of the estimates derived from two different NMHC ratios is suggested, calculated by the measurement of three different NMHC: A, B, C. If only the reaction with OH were to act on the mixing ratios in the air parcel, the two estimates will be related by the following linear expression (6) derived from equation (5).

$$\frac{\ln\left(\frac{[A]_t}{[B]_t}\right)}{Y} = \frac{\frac{(k_A-k_B)}{(k_C-k_B)}}{b}\frac{\ln\left(\frac{[C]_t}{[B]_t}\right)}{X} + \frac{\left[\ln\left(\frac{[A]_0}{[B]_0}\right) - \frac{(k_A-k_B)}{(k_C-k_B)}\ln\left(\frac{[C]_0}{[B]_0}\right)\right]}{a} \quad (6)$$

This linear relationship Y = b X+ a (6) eliminates the dependency on knowing ⟨[OH]⟩ and Δt and predicts a slope b, which is dependent only on the values for k_{OH} for the different NMHC. To reduce autocorrelation effects it is recommended that the longest-lived NMHC (here: ethane) be used as the denominator (B) and the more reactive compounds as numerators A and C (here: propane, n-butane, i-butane) (Parrish et al., 2004, 1992).

Using the mixing ratios of ethane, propane and n-butane, equation (6) was applied to the CARIBIC airborne measurements which had boundary layer contact (Section 2.4) during the *trans*-Africa flights (Fig. 8). The linear fit of the logarithmic NMHC-ratios correlates with $r^2 = 0.62$ for the different flights during this time period. The emission ratios for propane/ethane and n-butane/ethane for savanna burning, tropical forest burning estimated from the study from Akagi et al. (2011), and biofuel, estimated from the study of Andreae and Merlet (2001) were used as a basis to calculate OH-related loss processes. Also the 1:1 line representing pure dilution with air containing no NMHC is shown in the graph. The slope of 1.9 ± 0.2 of the linear fit of the CARIBIC samples is lower than the slope calculated for pure OH chemistry of 2.5 and is clearly higher than the slope of 1 for pure dilution. Therefore we surmise that the photochemical loss process is the main process, since the data fit is closer to the pure OH chemistry than to pure mixing, and that photochemistry is impacted by mixing processes with background air which shows very low mixing ratios of propane and n-butane. The samples taken in the SH (latitude < 0°N) fall furthest from the kinetic slope, indicating also input of cleaner air than for the NH samples. This is even more obvious when slopes for samples collected in each hemisphere are calculated, the NH air masses (n = 32) have a kinetic slope of 2.30 ± 0.2 ($R^2 = 0.83$) whereas the SH air masses (n = 22) have a kinetic slope of 1.53 ± 0.3 ($R^2 = 0.60$). Since the NH/SH OH ratio is considered to be close to one the overall reaction rate is the same in both hemispheres (Patra et al., 2014). The higher slope in the NH data (compared to the SH) must be the result of lower concentrations of NMHC (e.g. ethane and propane) in southern hemisphere background air. As is shown in paragraph 3.2.1, the background air still contains ethane and propane. A higher mixing ratio of propane/ethane in the NH background air compared to the SH would explain the higher slope in the NH.

To estimate the age of air an OH mixing ratio of 9.3 × 10^5 molec cm^{-3} (Spivakovsky et al., 2000), which is the mean OH mixing ratio between 12°N and 12°S at 200 hPa in January, was used with the emission ratios for propane/ethane and n-butane/ethane for savanna grassland burning of 0.15 and 0.02 (Akagi et al., 2011). The age of air was estimated for each ratio and is shown on a second

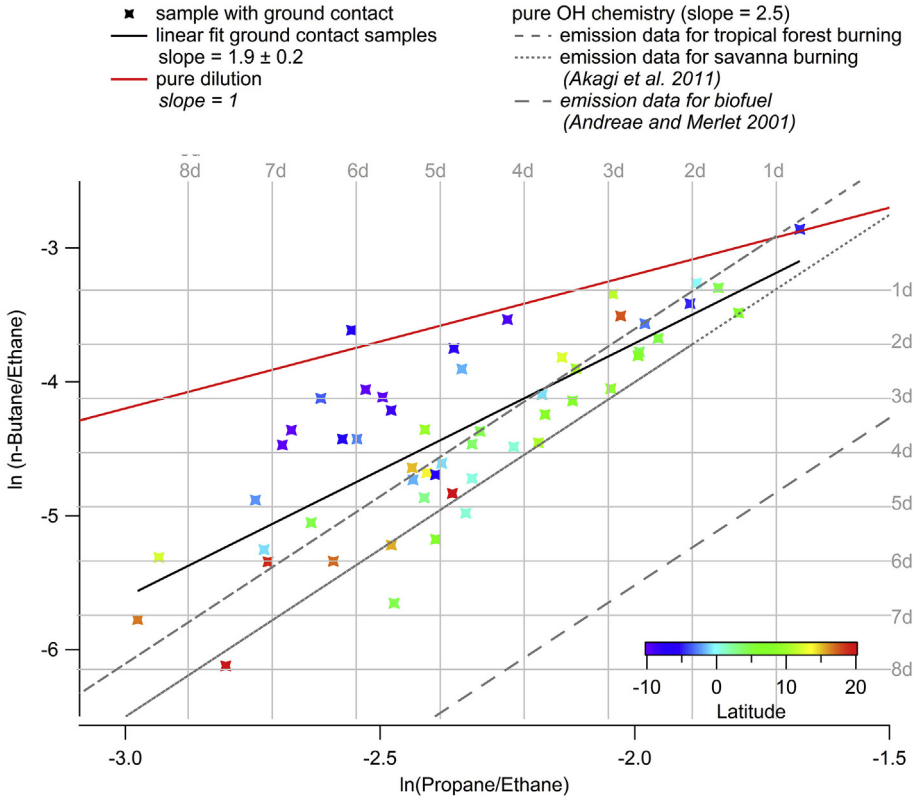

Fig. 8. Trace-tracer correlations for samples which had recent PBL contact (see Section 2.4). Samples are color-coded by sampling latitude. The slope is given as coefficient values ± one standard deviation.

axis in Fig. 8 (gray grid lines). The photochemical age Δt ranges between one and eight days for n-butane/ethane and one and nine days for propane/ethane. To estimate the kinetic slopes for pure OH chemistry we use a single-emission-time and no mixing model. With this we get for this calculation a well-defined age, and the photochemical ages calculated using the two ratios should be on the 1:1 line on the age axis (upper/right axis). The age estimates of the CARIBIC samples for the two different ratios differ from the 1:1 age-line, because of the mixing with background air. This mixing of background air is more obvious in SH air masses as mentioned before. Comparing the age estimates from NMHC-ratios with the background trajectory derived ages, of 88 h and 58 h, respectively it becomes apparent that the calculated photochemical age of air is 53% higher. Given the uncertainties involved, the agreement is reasonable. Uncertainties in OH mixing ratio of 25% correspond to uncertainty in transport time between 25% and 33% (Baker et al., 2011b). Moreover the uncertainty in used emission ratios derived from emission factors is similar. Therefore the estimate for the photochemical age of air derived by NMHC-ratios remains rather uncertain and the results for photochemical processing analysis are therefore only discussed qualitatively.

The concurrent measurement of O_3 and NMHC ratios can provide information about the net effect of photochemical O_3 production or loss (Parrish et al., 2004) if the effect of local influences and stratospheric O_3 can be ruled out. Local influences will be negligible at the 10–12 km cruising altitude. Also the impact of stratospheric O_3 is expected to be small. At tropical latitudes, the "high" mixing ratios of H_2O (200–300 ppm, Fig. 2) and CO (100–150 ppb) indicate prevailing upward transport and no descent from the stratosphere. In addition a filter for stratospherically influenced samples was used prior to data analysis (Section 2.3). Since O_3 in stratospheric air has a strong negative correlation with CO, such samples could be excluded by plotting ΔCO versus ΔO_3 (Fig. 14, supplement material) without finding any correlation. In Fig. 9 the O_3 concentration is plotted against the age of air, calculated based on the natural logarithm of propane/ethane. NOy mixing ratios measured are given as size of the symbols. This correlation plot is used to further elucidate the photochemical O_3 production (Parrish et al., 1992, 2004). For the whole dataset no significant correlation was found ($R^2 = 0.04$), when the NH and SH samples were separated, a positive very weak correlation was however found for the NH (slope = 1.63 ppb day^{-1}, $R^2 = 0.2$) and no correlation for SH ($R^2 = 0.02$). Within the dataset presented here we see O_3 production in the NH but not in the SH. Elevated NO_y mixing ratios in the NH, which are a proxy for higher NO_x conditions, explain this difference in O_3 production between the hemispheres. The O_3 production in BB plumes from Africa found in the NH is supported by several studies, e.g. O_3 production was found in BB outflow above the Atlantic during the SAFARI-92/TRACE A (Thompson et al., 1996), downwind from West Africa in the AMMA campaign (Real et al., 2010) and in undisturbed UT air masses (Andrés-Hernández et al., 2009) and in the NH tropics all year round by (Zahn et al., 2002).

4. Conclusion

Within the *trans*-African CARIBIC flight dataset taken between March 2009 and March 2011, elevated mixing ratios were observed for CO, CH_4, H_2O and aerosol particles. The elevated mixing ratios can be attributed in part to strong sources of BB between 0° and 10°N, which is related to the dry season north of the Equator during boreal winter. The elevated mixing ratios between the Equator and 10°S are a consequence of the stronger convection in the south due to the seasonal march of the ITCZ. The principally anthropogenically emitted halocarbons show a negative latitudinal gradient from the more industrialized NH to the SH.

Analyzing the NMHC data with positive matrix factorization (PMF) and comparing the results to the existing literature, three air mass types were found. Two of them could be attributed to trace gas emission sources (fossil fuels and BB), and one to background air. The NMHC mixing ratio pattern in the factor of background air followed the lifetimes of NMHC: ethane is the main component, followed by ethyne and propane with distinctly shorter lifetimes and benzene with even shorter lifetime (the lifetime of n-butane is so short that it is completely depleted in background air), suggesting this air has been in the free or upper troposphere for such a

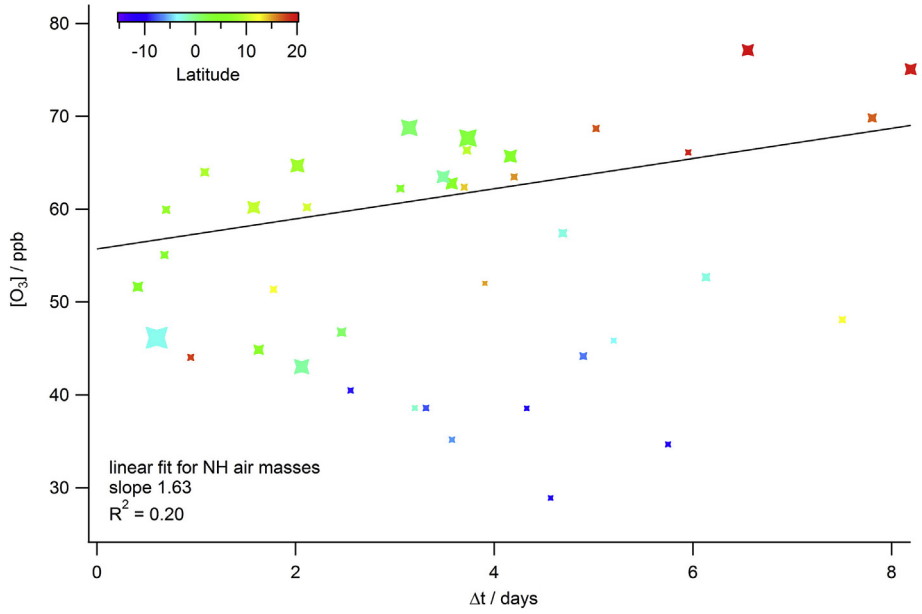

Fig. 9. Scatter plot O_3 vs. age of air ΔT (derived from ln propane/ethane). Samples are color-coded by sampling latitude. Sample size represents NOy mixing ratios measured within CARIBIC.

long time that all source information is lost. The comparison with in-situ measured compounds showed that the two emission related PMF sources, BB and fossil fuel, are correlated with CO and CH_4, which are tracers for pollution events and that the BB factor is correlated with accumulation mode particles (N_{140}), which are formed in BB. The background factor did not show a correlation, which supports the fact that background air has no measurable connection to its source emission and contains trace gases in amounts corresponding to their atmospheric lifetimes.

To investigate the emission sources in more detail, samples were filtered for recent contact to the boundary layer. From this subset of samples enhancement ratios ΔNMHC/ΔCO were calculated from NMHC-CO scatter plots. These enhancement ratios are often used for source identification of combustion processes. The calculated enhancement ratios from the air masses with boundary layer contact are comparable to enhancement ratios measured in a BB plume during an earlier CARIBIC phase 1 flight from Munich to Windhoek (Mühle, 2002), indicating that air masses with recent boundary layer contact are strongly influenced by BB emissions in this dataset. The comparison of the age corrected enhancement ratios with emission ratios measured for different classes of biomass in BB showed a good agreement with savanna and tropical forest burning emissions. Therefore we conclude that savanna and tropical forest burning are the main sources for BB emissions to the overall NMHC emissions from Africa, which is in agreement with the modeling results in Galanter et al. (2000).

NMHC ratios from boundary layer air masses are used to investigate photochemical processes. Using the ratios of ln(propane/ethane) and ln(n-butane/ethane) OH-photochemistry and mixing was investigated during the CARIBIC flights to South Africa. The slopes for the ln-ln plots are between the kinetic slopes for pure OH chemistry and mixing with background air. The two hemispheres show different patterns, whereby the SH air samples show a slope closer to the slope of mixing with clean background air, whilst the NH air samples have a slope closer to pure OH-photochemistry or mixing with background air still containing propane and ethane. This indicates that mixing with background air is either stronger in the south or that background air is cleaner, which is supported by the fact that the NH is generally more polluted than the SH. The investigation of O_3 production during the transport to the UT and the OH-oxidation in the Africa samples showed evidence of O_3 production, which is expected in the BB outflow.

Acknowledgments

The authors wish to thank the CARIBIC team, in particular Claus Koeppel for construction, installation and maintenance of the whole air sampling systems. CARIBIC is part of the European Research Infrastructure IAGOS (In-service Aircraft for a Global Observing System), which is financed partly by the German Ministry for Education and Research (BMBF 01LK1223). Operation of the CARIBIC observatory is possible through the support and cooperation of Lufthansa and Lufthansa Technik and Frankfurt and Munich airports.

Appendix A. Supplementary data

Supplementary data related to this article can be found at http://dx.doi.org/10.1016/j.atmosenv.2017.03.021.

References

Akagi, S.K., Yokelson, R.J., Wiedinmyer, C., Alvarado, M.J., Reid, J.S., Karl, T., Crounse, J.D., Wennberg, P.O., 2011. Emission factors for open and domestic biomass burning for use in atmospheric models. Atmos. Chem. Phys. 11, 4039–4072. http://dx.doi.org/10.5194/acp-11-4039-2011.

Andreae, M.O., Merlet, P., 2001. Emission of trace gases and aerosols from biomass burning. Glob. Biogeochem. Cycles 15, 955–966. http://dx.doi.org/10.1029/2000GB001382.

Andreae, M.O., Artaxo, P., Fischer, H., Freitas, S.R., Grégoire, J.-M., Hansel, A., Hoor, P., Kormann, R., Krejci, R., Lange, L., Lelieveld, J., Lindinger, W., Longo, K., Peters, W., de Reus, M., Scheeren, B., Silva Dias, M.A.F., Ström, J., van Velthoven, P.F.J., Williams, J., 2001. Transport of biomass burning smoke to the upper troposphere by deep convection in the equatorial region. Geophys. Res. Lett. 28, 951–954. http://dx.doi.org/10.1029/2000GL012391.

Andrés-Hernández, M.D., Kartal, D., Reichert, L., Burrows, J.P., Meyer Arnek, J., Lichtenstern, M., Stock, P., Schlager, H., 2009. Andres Hernandez Peroxy radical observation over west africa during AMMA 2006 photochemical activity in the outflow of convective systems 2009.pdf. Atmos. Chem. Phys. 9, 3681–3695. http://dx.doi.org/10.5194/acp-9-8103-2009.

Anomohanran, O., 2012. Determination of greenhouse gas emission resulting from gas flaring activities in Nigeria. Energy Policy 45, 666–670. http://dx.doi.org/10.1016/j.enpol.2012.03.018.

Assonov, S.S., Brenninkmeijer, C.A.M., Schuck, T., Umezawa, T., 2013. N2O as a tracer of mixing stratospheric and tropospheric air based on CARIBIC data with applications for CO2. Atmos. Environ. 79, 769–779. http://dx.doi.org/10.1016/j.atmosenv.2013.07.035.

Atkinson, R., 2003. Kinetics of the gas-phase reactions of OH radicals with alkanes and cycloalkanes. Atmos. Chem. Phys. 3, 2233–2307. http://dx.doi.org/10.5194/acp-3-2233-2003.

Baker, A.K., Beyersdorf, A.J., Doezema, L.A., Katzenstein, A., Meinardi, S., Simpson, I.J., Blake, D.R., Sherwood Rowland, F., 2008. Measurements of nonmethane hydrocarbons in 28 United States cities. Atmos. Environ. 42, 170–182. http://dx.doi.org/10.1016/j.atmosenv.2007.09.007.

Baker, A.K., Slemr, F., Brenninkmeijer, C.A.M., 2010. Analysis of non-methane hydrocarbons in air samples collected aboard the CARIBIC passenger aircraft. Atmos. Meas. Tech. 3, 311–321. http://dx.doi.org/10.5194/amt-3-311-2010.

Baker, A.K., Rauthe-Schöch, A., Schuck, T.J., Brenninkmeijer, C.a.M., Van Velthoven, P.F.J., Wisher, A., Oram, D.E., 2011a. Investigation of chlorine radical chemistry in the Eyjafjallajökull volcanic plume using observed depletions in non-methane hydrocarbons. Geophys. Res. Lett. 38 http://dx.doi.org/10.1029/2011GL047571 n/a-n/a.

Baker, A.K., Schuck, T.J., Slemr, F., van Velthoven, P.F.J., Zahn, A., Brenninkmeijer, C.a.M., 2011b. Characterization of non-methane hydrocarbons in Asian summer monsoon outflow observed by the CARIBIC aircraft. Atmos. Chem. Phys. 11, 503–518. http://dx.doi.org/10.5194/acp-11-503-2011.

Baker, A.K., Schuck, T.J., Brenninkmeijer, C.a.M., Rauthe-Schöch, A., Slemr, F., Van Velthoven, P.F.J., Lelieveld, J., 2012. Estimating the contribution of monsoon-related biogenic production to methane emissions from South Asia using CARIBIC observations. Geophys. Res. Lett. 39, 6–11. http://dx.doi.org/10.1029/2012GL051756.

Baker, A.K., Sauvage, C., Thorenz, U.R., van Velthoven, P., Oram, D.E., Zahn, A., Brenninkmeijer, C.A.M., Williams, J., 2016. Evidence for strong, widespread chlorine radical chemistry associated with pollution outflow from continental Asia. Sci. Rep. 6, 36821. http://dx.doi.org/10.1038/srep36821.

Bechara, J., Borbon, A., Jambert, C., Colomb, A., Perros, P.E., 2010. Evidence of the impact of deep convection on reactive Volatile Organic Compounds in the upper tropical troposphere during the AMMA experiment in West Africa. Atmos. Chem. Phys. 10, 10321–10334. http://dx.doi.org/10.5194/acp-10-10321-2010.

Blake, N.J., Blake, D.R., Sive, B.C., Chen, T., Rowland, F.S., Collins, J.E., Sachse, G.W., Anderson, B.E., 1996. Biomass burning emissions and vertical distribution of atmospheric methyl halides and other reduced carbon gases in the South Atlantic region. J. Geophys. Res. Atmos. 101, 24151–24164. http://dx.doi.org/10.1029/96JD00561.

Brenninkmeijer, C.A.M., Crutzen, P., Boumard, F., Dauer, T., Dix, B., Ebinghaus, R., Filippi, D., Fischer, H., Franke, H., Frieβ, U., Heintzenberg, J., Helleis, F., Hermann, M., Kock, H.H., Koeppel, C., Lelieveld, J., Leuenberger, M., Martinsson, B.G., Miemczyk, S., Moret, H.P., Nguyen, H.N., Nyfeler, P., Oram, D., O'Sullivan, D., Penkett, S., Platt, U., Pupek, M., Ramonet, M., Randa, B., Reichelt, M., Rhee, T.S., Rohwer, J., Rosenfeld, K., Scharffe, D., Schlager, H., Schumann, U., Slemr, F., Sprung, D., Stock, P., Thaler, R., Valentino, F., van Velthoven, P., Waibel, A., Wandel, A., Waschitschek, K., Wiedensohler, A., Xueref-Remy, I., Zahn, A., Zech, U., Ziereis, H., 2007. Civil Aircraft for the regular investigation of the atmosphere based on an instrumented container: the new CARIBIC system. Atmos. Chem. Phys. 7, 4953–4976. http://dx.doi.org/10.5194/acp-7-4953-2007.

Brown, S.G., Eberly, S., Paatero, P., Norris, G.A., 2015. Methods for estimating uncertainty in PMF solutions: examples with ambient air and water quality data and guidance on reporting PMF results. Sci. Total Environ. 518–519, 626–635. http://dx.doi.org/10.1016/j.scitotenv.2015.01.022.

Buzcu, B., Fraser, M.P., 2006. Source identification and apportionment of volatile organic compounds in Houston, TX. Atmos. Environ. 40, 2385–2400. http://dx.doi.org/10.1016/j.atmosenv.2005.12.020.

Capes, G., Johnson, B., McFiggans, G., Williams, P.I., Haywood, J., Coe, H., 2008. Aging of biomass burning aerosols over West Africa: aircraft measurements of chemical composition, microphysical properties, and emission ratios. J. Geophys. Res. 113, D00C15. http://dx.doi.org/10.1029/2008JD009845.

Chan, S.H., Wang, H.M., 2000. Effect of natural gas composition on autothermal fuel

reforming products. Fuel Process. Technol 64, 221–239. http://dx.doi.org/10.1016/S0378-3820(00)00065-5.
Crutzen, P.J., Andreae, M.O., 1990. Biomass burning in the tropics: impact on atmospheric chemistry and biogeochemical cycles. Science 250 (80), 1669–1678. http://dx.doi.org/10.1126/science.250.4988.1669.
de Gouw, J.A., Warneke, C., Scheeren, H.A., van der Veen, C., Bolder, M., Scheele, M.P., Williams, J., Wong, S., Lange, L., Fischer, H., Lelieveld, J., 2001. Overview of the trace gas measurements on board the Citation aircraft during the intensive field phase of INDOEX. J. Geophys. Res. Atmos. 106, 28453–28467. http://dx.doi.org/10.1029/2000JD900810.
Dyroff, C., Zahn, A., Christner, E., Forbes, R., Tompkins, A.M., van Velthoven, P.F.J., 2015. Comparison of ECMWF analysis and forecast humidity data with CARIBIC upper troposphere and lower stratosphere observations. Q. J. R. Meteorol. Soc. 141, 833–844. http://dx.doi.org/10.1002/qj.2400.
Dyroff, C., Zahn, A., Sanati, S., Christner, E., Rauthe-Schöch, A., Schuck, T.J., 2014. Tunable diode laser in-situ CH_4 measurements aboard the CARIBIC passenger aircraft: instrument performance assessment. Atmos. Meas. Tech. 7, 743–755. http://dx.doi.org/10.5194/amt-7-743-2014.
Leedham Elvidge, E.C., Oram, D.E., Laube, J.C., Baker, A.K., Montzka, S.A., Humphrey, S., O'Sullivan, D.A., Brenninkmeijer, C.A.M., 2015. Increasing concentrations of dichloromethane, CH2Cl2, inferred from CARIBIC air samples collected 1998–2012. Atmos. Chem. Phys. 15, 1939–1958. http://dx.doi.org/10.5194/acp-15-1939-2015.
Fishman, J., Hoell, J.M., Bendura, R.D., McNeal, R.J., Kirchhoff, V.W.J.H., 1996. NASA GTE TRACE a experiment (September–October 1992): overview. J. Geophys. Res. 101, 23865. http://dx.doi.org/10.1029/96JD00123.
Galanter, M., Levy, H., Carmichael, G.R., 2000. Impacts of biomass burning on tropospheric CO, NO x, and O 3. J. Geophys. Res. 105, 6633. http://dx.doi.org/10.1029/1999JD901113.
Gebhardt, S., Colomb, A., Hofmann, R., 2008. Halogenated organic species over the tropical South American rainforest. Atmos. Chem. … 2050 3185–3197. http://dx.doi.org/10.5194/acp-8-3185-2008.
Giglio, L., Descloitres, J., Justice, C.O., Kaufman, Y.J., 2003. An enhanced contextual fire detection algorithm for MODIS. Remote Sens. Environ. 87, 273–282. http://dx.doi.org/10.1016/S0034-4257(03)00184-6.
Goudie, A.S., 1996. Climate: past and present. Oxford. In: Adams, W.M., Goudie, A.S., Orme, A.R. (Eds.), The Physical Geography of Africa, pp. 34–59.
Gros, V., Bonsang, B., Martin, D., Novelli, P.C., Kazan, V., 1999. Carbon monoxide short term measurements at Amsterdam island: estimations of biomass burning emission rates. Chemosph. - Glob. Chang. Sci. 1, 163–172. http://dx.doi.org/10.1016/S1465-9972(99)00009-4.
Guenther, A., Otter, L., Zimmerman, P., Greenberg, J., Scholes, R., Scholes, M., 1996. Biogenic hydrocarbon emissions from southern African savannas. J. Geophys. Res. 101, 25859. http://dx.doi.org/10.1029/96JD02597.
Haywood, J.M., Pelon, J., Formenti, P., Bharmal, N.A., Brooks, M.E., Capes, G., Chazette, P., Chou, C., Christopher, S.A., Coe, H., Cuesta, J., Derimian, Y., Desboeufs, K., Greed, G., Harrison, M., Heese, B., Highwood, E.J., Johnson, B., Mallet, M., Marticorena, B., Marsham, J., Milton, S., Myhre, G., Osborne, S.R., Parker, D.J., Rajot, J.L., Schulz, M., Slingo, A., Tanré, D., Tulet, P., 2008. Overview of the dust and biomass-burning experiment and African monsoon multidisciplinary analysis special observing period-0. J. Geophys. Res. Atmos. 113, 1–20. http://dx.doi.org/10.1029/2008JD010077.
Heintzenberg, J., Hermann, M., Theiss, D., 2003. Out of Africa: high aerosol concentrations in the upper troposphere over Africa. Atmos. Chem. Phys. 3, 1191–1198. http://dx.doi.org/10.5194/acp-3-1191-2003.
Heintzenberg, J., Hermann, M., Weigelt, A., Clarke, A., Kapustin, V., Anderson, B., Thornhill, K., Van Velthoven, P., Zahn, A., Brenninkmeijer, C., 2011. Near-global aerosol mapping in the upper troposphere and lowermost stratosphere with data from the CARIBIC project. Tellus B 63, 875–890. http://dx.doi.org/10.1111/j.1600-0889.2011.00578.x.
Helmig, D., Tanner, D.M., Honrath, R.E., Owen, R.C., Parrish, D.D., 2008. Nonmethane hydrocarbons at Pico mountain, azores: 1. Oxidation chemistry in the north atlantic region. J. Geophys. Res. Atmos. 113, 1–16. http://dx.doi.org/10.1029/2007JD008930.
Hermann, M., 2003. Meridional distributions of aerosol particle number concentrations in the upper troposphere and lower stratosphere obtained by Civil Aircraft for Regular Investigation of the Atmosphere Based on an Instrument Container (CARIBIC) flights. J. Geophys. Res. 108, 4114. http://dx.doi.org/10.1029/2001JD001077.
Hermann, M., Wiedensohler, A., 2001. Counting efficiency of condensation particle counters at low-pressures with illustrative data from the upper troposphere. J. Aerosol Sci. 32, 975–991. http://dx.doi.org/10.1016/S0021-8502(01)00037-4.
Hermann, M., Weigelt, A., Assmann, D., Pfeifer, S., Müller, T., Conrath, T., Voigtländer, J., Heintzenberg, J., Wiedensohler, A., Martinsson, B.G., Deshler, T., Brenninkmeijer, C.A.M., Zahn, A., 2016. An optical particle size spectrometer for aircraft-borne measurements in IAGOS-CARIBIC. Atmos. Meas. Tech. Discuss. 9, 2179–2194. http://dx.doi.org/10.5194/amt-9-2179-2016, 2016.
Honrath, R.E., Helmig, D., Owen, R.C., Parrish, D.D., Tanner, D.M., 2008. Nonmethane hydrocarbons at Pico Mountain, Azores: 2. Event-specific analyses of the impacts of mixing and photochemistry on hydrocarbon ratios. J. Geophys. Res. Atmos. 113, 1–12. http://dx.doi.org/10.1029/2008JD009832.
Hopkins, J.R., Evans, M.J., Lee, J.D., Lewis, A.C.H., Marsham, J., McQuaid, J.B., Parker, D.J., Stewart, D.J., Reeves, C.E., Purvis, R.M., 2009. Direct estimates of emissions from the megacity of Lagos. Atmos. Chem. Phys. 9, 8471–8477. http://dx.doi.org/10.5194/acp-9-8471-2009.
Ishijima, K., Patra, P.K., Takigawa, M., Machida, T., Matsueda, H., Sawa, Y., Steele, L.P., Krummel, P.B., Langenfelds, R.L., Aoki, S., Nakazawa, T., 2010. Stratospheric influence on the seasonal cycle of nitrous oxide in the troposphere as deduced from aircraft observations and model simulations. J. Geophys. Res. 115, D20308. http://dx.doi.org/10.1029/2009JD013322.
Johnson, B.T., Osborne, S.R., Haywood, J.M., Harrison, M.A.J., 2008. Aircraft measurements of biomass burning aerosol over West Africa during DABEX. J. Geophys. Res. 113, D00C06. http://dx.doi.org/10.1029/2007JD009451.
Karl, T., Apel, E., Hodzic, A., Riemer, D.D., Blake, D.R., Wiedinmyer, C., 2009. Emissions of volatile organic compounds inferred from airborne flux measurements over a megacity. Atmos. Chem. Phys. 9, 271–285. http://dx.doi.org/10.5194/acp-9-271-2009.
Khalil, M.A.K., Rasmussen, R.A., 1990. The global cycle of carbon monoxide: trends and mass balance. Chemosphere 20, 227–242. http://dx.doi.org/10.1016/0045-6535(90)90098-E.
Khalil, M.A.K., Rasmussen, R.A., 1999. Atmospheric methyl chloride. Atmos. Environ. 33, 1305–1321. http://dx.doi.org/10.1016/S1352-2310(98)00234-9.
Kirschke, S., Bousquet, P., Ciais, P., Saunois, M., Canadell, J.G., Dlugokencky, E.J., Bergamaschi, P., Bergmann, D., Blake, D.R., Bruhwiler, L., Cameron-Smith, P., Castaldi, S., Chevallier, F., Feng, L., Fraser, A., Heimann, M., Hodson, E.L., Houweling, S., Josse, B., Fraser, P.J., Krummel, P.B., Lamarque, J.-F., Langenfelds, R.L., Le Quéré, C., Naik, V., O'Doherty, S., Palmer, P.I., Pison, I., Plummer, D., Poulter, B., Prinn, R.G., Rigby, M., Ringeval, B., Santini, M., Schmidt, M., Shindell, D.T., Simpson, I.J., Spahni, R., Steele, L.P., Strode, S.A., Sudo, K., Szopa, S., van der Werf, G.R., Voulgarakis, A., van Weele, M., Weiss, R.F., Williams, J.E., Zeng, G., 2013. Three decades of global methane sources and sinks. Nat. Geosci. 6, 813–823. http://dx.doi.org/10.1038/ngeo1955.
Köppe, M., Hermann, M., Brenninkmeijer, C.A.M., Heintzenberg, J., Schlager, H., Schuck, T., Slemr, F., Sprung, D., van Velthoven, P.F.J., Wiedensohler, A., Zahn, A., Ziereis, H., 2009. Origin of aerosol particles in the mid-latitude and subtropical upper troposphere and lowermost stratosphere from cluster analysis of CARIBIC data. Atmos. Chem. Phys. 9, 8413–8430. http://dx.doi.org/10.5194/acp-9-8413-2009.
Laakso, L., Laakso, H., Aalto, P.P., Keronen, P., Petäjä, T., Nieminen, T., Pohja, T., Siivola, E., Kulmala, M., Kgabi, N., Molefe, M., Mabaso, D., Phalatse, D., Pienaar, K., Kerminen, V.-M., 2008. Basic characteristics of atmospheric particles, trace gases and meteorology in a relatively clean Southern African Savannah environment. Atmos. Chem. Phys. 8, 4823–4839. http://dx.doi.org/10.5194/acp-8-4823-2008.
Laturnus, F., Haselmann, K.F., Borch, T., Grøn, C., 2002. Terrestrial natural sources of trichloromethane (chloroform, CHCl3) — an overview. Biogeochemistry 60, 121–139. http://dx.doi.org/10.1023/A:1019887505651.
Leedham, E.C., Hughes, C., Keng, F.S.L., Phang, S.-M., Malin, G., Sturges, W.T., 2013. Emission of atmospherically significant halocarbons by naturally occurring and farmed tropical macroalgae. Biogeosciences 10, 3615–3633. http://dx.doi.org/10.5194/bg-10-3615-2013.
Li, J., Xie, S.D., Zeng, L.M., Li, L.Y., Li, Y.Q., Wu, R.R., 2015. Characterization of ambient volatile organic compounds and their sources in Beijing, before, during, and after Asia-Pacific Economic Cooperation China 2014. Atmos. Chem. Phys. 15, 7945–7959. http://dx.doi.org/10.5194/acp-15-7945-2015.
Liu, C., Zipser, E.J., 2005. Global distribution of convection penetrating the tropical tropopause. J. Geophys. Res. Atmos. 110, 1–12. http://dx.doi.org/10.1029/2005JD006063.
Mari, C.H., Cailley, G., Corre, L., Saunois, M., Attié, J.L., Thouret, V., Stohl, A., 2008. Tracing biomass burning plumes from the Southern Hemisphere during the AMMA 2006 wet season experiment. Atmos. Chem. Phys. 8, 3951–3961. http://dx.doi.org/10.5194/acp-8-3951-2008.
Matsuki, A., Quennehen, B., Schwarzenboeck, A., Crumeyrolle, S., Venzac, H., Laj, P., Gomes, L., 2010. Temporal and vertical variations of aerosol physical and chemical properties over West Africa: AMMA aircraft campaign in summer 2006. Atmos. Chem. Phys. 10, 8437–8451. http://dx.doi.org/10.5194/acp-10-8437-2010.
Mauzerall, D.L., Logan, J.A., Jacob, D.J., Anderson, B.E., Blake, D.R., Bradshaw, J.D., Heikes, B., Sachse, G.W., Singh, H., Talbot, B., 1998. Photochemistry in biomass burning plumes and implications for tropospheric ozone over the tropical South Atlantic. J. Geophys. Res. 103, 8401. http://dx.doi.org/10.1029/97JD02612.
Montzka, S.A., Reimann, S., 2010. Ozone-depleting Substances (ODSs) and Related Chemicals, p. 1, 108.
Mühle, J., Brenninkmeijer, C.A.M., Rhee, T.S., Slemr, F., Oram, D.E., Penkett, S.A., Zahn, A., 2002. Biomass burning and fossil fuel signatures in the upper troposphere observed during a CARIBIC flight from Namibia to Germany. Geophys. Res. Lett. 29, 2–5. http://dx.doi.org/10.1029/2002GL015764.
Murdock, G.P., 1959. Africa: its Peoples and Their Culture History: Maps, Africa: its Peoples and Their Culture History. McGraw-Hill.
Nguyen, H., Duvel, J.-P., 2008. Synoptic wave perturbations and convective systems over equatorial africa. J. Clim. 21, 6372–6388. http://dx.doi.org/10.1175/2008JCLI2409.1.
Paatero, P., Tapper, U., 1994. Positive matrix factorization - a nonnegative factor model with optimal utilization of error estimates of data values. Environmetrics 5, 111–126. http://dx.doi.org/10.1002/env.3170050203.
Paatero, P., Eberly, S., Brown, S.G., Norris, G.A., 2014. Methods for estimating uncertainty in factor analytic solutions. Atmos. Meas. Tech. 7, 781–797. http://dx.doi.org/10.5194/amt-7-781-2014.
Parrish, D.D., Hahn, C.J., Williams, E.J., Norton, R.B., Fehsenfeld, F.C., Singh, H.B., Shetter, J.D., Gandrud, B.W., Ridley, B.A., 1992. Indications of Photochemical

Histories of Pacific Air Masses from Measurements of Atmospheric Trace Species at Point Arena, California, p. 97. http://dx.doi.org/10.1029/93JD01416.
Parrish, D.D., Trainer, M., Young, V., Goldan, P.D., Kuster, W.C., Jobson, B.T., Fehsenfeld, F.C., Lonneman, W.A., Zika, R.D., Farmer, C.T., Riemer, D.D., Rodgers, M.O., 1998. Internal consistency tests for evaluation of measurements of anthropogenic hydrocarbons in the troposphere. J. Geophys. Res. 103, 22339. http://dx.doi.org/10.1029/98JD01364.
Parrish, D.D., Dunlea, E.J., Atlas, E.L., Schauffler, S., Donnelly, S., Stroud, V., Goldstein, A.H., Millet, D.B., McKay, M., Jaffe, D.A., Price, H.U., Hess, P.G., Flocke, F., Roberts, J.M., 2004. Changes in the photochemical environment of the temperate North Pacific troposphere in response to increased Asian emissions. J. Geophys. Res. D. Atmos. 109, 1–16. http://dx.doi.org/10.1029/2004JD004978.
Parrish, D.D., Stohl, A., Forster, C., Atlas, E.L., Blake, D.R., Goldan, P.D., Kuster, W.C., de Gouw, J.A., 2007. Effects of mixing on evolution of hydrocarbon ratios in the troposphere. J. Geophys. Res. Atmos. 112, 1–17. http://dx.doi.org/10.1029/2006JD007583.
Patra, P.K., Krol, M.C., Montzka, S.A., Arnold, T., Atlas, E.L., Lintner, B.R., Stephens, B.B., Xiang, B., Elkins, J.W., Fraser, P.J., Ghosh, A., Hintsa, E.J., Hurst, D.F., Ishijima, K., Krummel, P.B., Miller, B.R., Miyazaki, K., Moore, F.L., Mühle, J., O'Doherty, S., Prinn, R.G., Steele, L.P., Takigawa, M., Wang, H.J., Weiss, R.F., Wofsy, S.C., Young, D., 2014. Observational evidence for interhemispheric hydroxyl-radical parity. Nature 513, 219–223. http://dx.doi.org/10.1038/nature13721.
Real, E., Orlandi, E., Law, K.S., Fierli, F., Josset, D., Cairo, F., Schlager, H., Borrmann, S., Kunkel, D., Volk, C.M., McQuaid, J.B., Stewart, D.J., Lee, J., Lewis, A.C., Hopkins, J.R., Ravegnani, F., Ulanovski, A., Liousse, C., 2010. Cross-hemispheric transport of central African biomass burning pollutants: implications for downwind ozone production. Atmos. Chem. Phys. 10, 3027–3046. http://dx.doi.org/10.5194/acp-10-3027-2010.
Roberts, G., Wooster, M.J., Lagoudakis, E., 2009. Annual and diurnal african biomass burning temporal dynamics. Biogeosciences 6, 849–866. http://dx.doi.org/10.5194/bg-6-849-2009.
Sauvage, B., Thouret, V., Cammas, J.P., Brioude, J., Nédélec, P., Mari, C., 2007. Meridional ozone gradients in the African upper troposphere. Geophys. Res. Lett. 34, 1–5. http://dx.doi.org/10.1029/2006GL028542.
Scharffe, D., Slemr, F., Brenninkmeijer, C.A.M., Zahn, A., 2012. Carbon monoxide measurements onboard the CARIBIC passenger aircraft using UV resonance fluorescence. Atmos. Meas. Tech. 5, 1753–1760. http://dx.doi.org/10.5194/amt-5-1753-2012.
Scheele, M.P., Siegmund, P.C., Van Velthoven, P.F.J., 1996. Sensitivity of trajectories to data resolution and its dependence on the starting point: in or outside a tropopause fold. Meteorol. Appl. 3, 267–273. http://dx.doi.org/10.1002/met.5060030308.
Scheeren, H.A., Lelieveld, J., Roelofs, G.J., Williams, J., Fischer, H., de Reus, M., de Gouw, J.A., Warneke, C., Holzinger, R., Schlager, H., Klüpfel, T., Bolder, M., van der Veen, C., Lawrence, M., 2003. The impact of monsoon outflow from India and Southeast Asia in the upper troposphere over the eastern Mediterranean. Atmos. Chem. Phys. 3, 1589–1608. http://dx.doi.org/10.5194/acp-3-1589-2003.
Scholes, M., Andreae, M.O., 2000. Biogenic and pyrogenic emissions from africa and their impact on the global atmosphere. AMBIO A J. Hum. Environ. 29, 23–29. http://dx.doi.org/10.1579/0044-7447-29.1.23.
Schuck, T.J., Brenninkmeijer, C.A.M., Slemr, F., Xueref-Remy, I., Zahn, A., 2009. Greenhouse gas analysis of air samples collected onboard the CARIBIC passenger aircraft. Atmos. Meas. Tech. 2, 449–464. http://dx.doi.org/10.5194/amt-2-449-2009.
Schuck, T.J., Ishijima, K., Patra, P.K., Baker, A.K., Machida, T., Matsueda, H., Sawa, Y., Umezawa, T., Brenninkmeijer, C.A.M., Lelieveld, J., 2012. Distribution of methane in the tropical upper troposphere measured by CARIBIC and CONTRAIL aircraft. J. Geophys. Res. Atmos. 117 http://dx.doi.org/10.1029/2012JD018199 n/a-n/a.
Shao, P., An, J., Xin, J., Wu, F., Wang, J., Ji, D., Wang, Y., 2016. Source apportionment of VOCs and the contribution to photochemical ozone formation during summer in the typical industrial area in the Yangtze River Delta, China. Atmos. Res. 176–177, 64–74. http://dx.doi.org/10.1016/j.atmosres.2016.02.015.
Simpson, I.J., 2004. Long-term decrease in the global atmospheric burden of tetrachloroethene (C 2 Cl 4). Geophys. Res. Lett. 31, L08108. http://dx.doi.org/10.1029/2003GL019351.
Song, Y., Shao, M., Liu, Y., Lu, S., Kuster, W., Goldan, P., Xie, S., 2007. Source apportionment of ambient volatile organic compounds in Beijing. Environ. Sci. Technol. 41, 4348–4353. http://dx.doi.org/10.1021/es0625982.
Spivakovsky, C.M., Logan, J.A., Montzka, S.A., Balkanski, Y.J., Foreman-Fowler, M., Jones, D.B.A., Horowitz, L.W., Fusco, A.C., Brenninkmeijer, C.A.M., Prather, M.J., Wofsy, S.C., McElroy, M.B., 2000. Three-dimensional climatological distribution of tropospheric OH: update and evaluation. J. Geophys. Res. Atmos. 105, 8931–8980. http://dx.doi.org/10.1029/1999JD901006.
Swap, R.J., Annegarn, H.J., Timothy, S., King, M.D., Platnick, S., Privette, J.L., Scholes, R.J., 2003. Africa burning: a thematic analysis of the southern african regional science initiative (SAFARI 2000). J. Geophys. Res. 108, 1–15. http://dx.doi.org/10.1029/2003JD003747.
Thompson, A.M., Diab, R.D., Bodeker, G.E., Zunckel, M., Coetzee, G.J.R., Archer, C.B., McNamara, D.P., Pickering, K.E., Combrink, J., Fishman, J., Nganga, D., 1996. Ozone over southern Africa during SAFARI-92/TRACE A. J. Geophys. Res. 101, 23793. http://dx.doi.org/10.1029/95JD02459.
Tubiello, F.N., Salvatore, M., Rossi, S., Ferrara, A., Fitton, N., Smith, P., 2013. The FAOSTAT database of greenhouse gas emissions from agriculture. Environ. Res. Lett. 8, 15009. http://dx.doi.org/10.1088/1748-9326/8/1/015009.
Umezawa, T., Baker, A.K., Oram, D., Sauvage, C., O'Sullivan, D., Rauthe-Schöch, A., Montzka, S.A., Zahn, A., Brenninkmeijer, C.A.M., 2014. Methyl chloride in the upper troposphere observed by the CARIBIC passenger aircraft observatory: large-scale distributions and Asian summer monsoon outflow. J. Geophys. Res. Atmos. 119, 5542–5558. http://dx.doi.org/10.1002/2013JD021396.
U.S. EPA, 2014. EPA Positive Matrix Factorization (PM F) 5.0, User Guide (Washington DC).
van Velthoven, P.F.J., 2016. Meteorological analysis of CARIBIC by KNMI [WWW Document]. http//projects.knmi.nl/campaignsupport/CARIBIC/, 2016.
Waliser, D.E., Gautier, C., 1993. A satellite-derived climatology of the ITCZ. J. Clim. 6, 2162–2174. http://dx.doi.org/10.1175/1520-0442(1993)006<2162:ASDCOT>2.0.CO;2.
Williams, J., Fischer, H., Wong, S., Crutzen, P.J., Scheele, M.P., Lelieveld, J., 2002. Near equatorial CO and O3 profiles over the Indian Ocean during the winter monsoon: High O3 levels in the middle troposphere and interhemispheric exchange. J. Geophys. Res. Atmos. 107 http://dx.doi.org/10.1029/2001JD001126. INX2 6-1-INX2 6-13.
Wisher, A., Oram, D.E., Laube, J.C., Mills, G.P., van Velthoven, P., Zahn, A., Brenninkmeijer, C.A.M., 2014. Very short-lived bromomethanes measured by the CARIBIC observatory over the north atlantic, africa and southeast asia during 2009–2013. Atmos. Chem. Phys. 14, 3557–3570. http://dx.doi.org/10.5194/acp-14-3557-2014.
Zahn, A., Brenninkmeijer, C.A.M., Asman, W.A.H., Crutzen, P.J., Heinrich, G., Fischer, H., Cuijpers, J.W.M., van Velthoven, P.F.J., 2002. Budgets of O 3 and CO in the upper troposphere: CARIBIC passenger aircraft results 1997-2001. J. Geophys. Res. Atmos. 107 http://dx.doi.org/10.1029/2001JD001529. ACH 6-1–ACH 6-20.